Institute of Paper Science and Technology
Atlanta, Georgia

IPST TECHNICAL PAPER SERIES

NUMBER 346

PRINCIPLES OF HYDRODYNAMIC INSTABILITY IN COATING SYSTEMS

CYRUS K. AIDUN

MARCH, 1990

Principles of Hydrodynamic Instability in Coating Systems

Cyrus K. Aidun

For presentation at the
1990 TAPPI Coating Conference, Boston, MA
May 13-16

PRINCIPLES OF HYDRODYNAMIC INSTABILITY IN COATING SYSTEMS

Cyrus K. Aidun
Assistant Professor
Institute of Paper Science and Technology
575 14th Street, N.W.
Atlanta, Georgia 30318

ABSTRACT

With the development and installation of new high speed paper machines the coating technology faces a new class of challenging problems. Coaters are expected to operate in excess of 5000 fpm where coating rheology and flow instability become critical issues. The ideal flow in a coating device is steady state and two dimensional, that is, no velocity components or momentum transfer in the cross machine direction. Any deviations from this flow condition often result in poor coated surface properties and cannot be tolerated. The demand for high operating speeds and better surface quality creates new challenges which require advanced technological and scientific approaches. Since paper coating involves application of complex fluids at high speeds and under extreme flow conditions, the fluid mechanics and instability problems which arise are often unique and require fundamental and in-depth analysis.

The purpose of this paper is to outline and review practical techniques for analyzing and predicting flow instability in coating systems. General principles of flow instability are outlined in the first section and examples of flow instability in coating systems are discussed in section II. Flow through coating devices as nonlinear dynamical systems can only behave in a specific and consistent manner according to the basic physical principles. Knowing the fundamental physical and dynamical principles (e.g., general behavior and transitions between steady and time-periodic states) can help us to more efficiently deduce and interpret information from experiments or computational analysis of instability issues in coating systems. Therefore, a section at the end is devoted to principles of nonlinear dynamics. Simple mathematical demonstrations and examples are included throughout the paper for the sake of clarity and also to provide simple but practical working tools.

KEYWORDS

Fluid mechanics, blade coating, hydrodynamic stability, flow patterns in coating systems.

I. INTRODUCTION

"Yet not every solution of the equations of motion, even if it is exact, can actually occur in Nature. The flows that occur in Nature must not only obey the equations (conservation principles) *of fluid dynamics, but also be stable."*

- Landau and Lifshitz (1959)

Hydrodynamic instability has been the central issue in the study of the physics of fluid motion for more than a century. This topic has received considerable attention in the past from scientists and engineers and continues to be one of the dominating issues in the field of continuum mechanics. The reason for its importance stems from the fact that a flow system can satisfy all of the fluid mechanics conservation principles and yet be unstable and non-existent in nature.

In general, every laminar flow pattern will become unstable at some critical flow parameter and undergo a transition to a qualitatively different flow. The new flow system could be steady, periodic, or unsteady. Here, the key issue is transition between qualitatively different systems or states.

Study of flow instability started in the nineteenth century with physicists such as Helmholtz, Kelvin, Rayleigh, and Reynolds. The classical experiments of Osborne Reynolds (1883) on the flow in a pipe is perhaps the most well-known study in fluid mechanics. In these experiments, water was drawn out of a large glass tank through a circular tube while a streak of highly colored water entered simultaneously with the clear water. The results of these experiments in Reynolds' own words are as follows:

a) *When the velocities were sufficiently low, the streak of colour extended a beautiful straight line through the tube, Figure I.1a.*

b) *If the water in the tank had not quite settled to rest, at sufficiently low velocities, the streak would shift about the tube, but there was no appearance of sinuosity.*

c) *As the velocity was increased by small stages, at some point in the tube, ..., the colour band would all at once mix up with the surrounding water, and fill the rest of the tube with a mass of coloured water, as in Figure I.1b. ... On viewing the tube by a light of an electric spark, the mass of colour resolved itself into a mass of more*

or less distinct curls, showing eddies, as in Figure I.1c. ... the critical velocity was very sensitive to disturbance in the water before entering the tube. ... This at once suggested the idea that the condition might be one of instability for disturbance of certain magnitude and stable for smaller disturbances.

—Reynolds (1883)

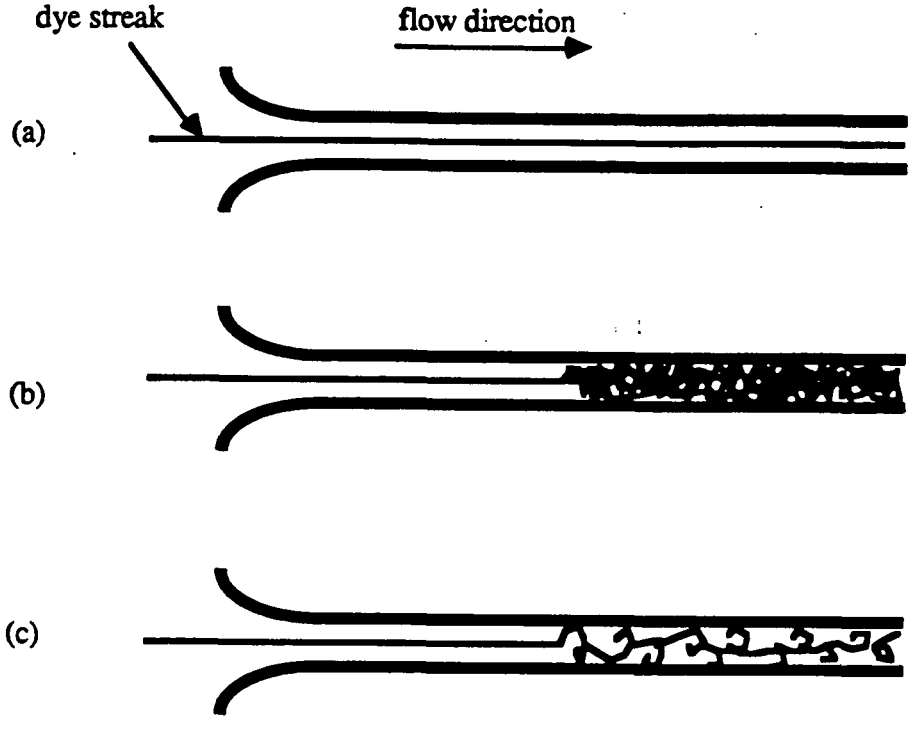

Figure I.1 (a) Laminar flow in a pipe; (b) Transition to turbulent flow in a pipe; and (c) Transition to turbulent flow as seen when illuminated by a spark. (From Reynolds, 1883.)

Reynolds repeated these experiments with different diameter tubes and established a dimensionless parameter, VD/ν, based on velocity, V, diameter, D, and kinematic viscosity, ν. This parameter, which is now referred to as the Reynolds number, defines the class of dynamically similar flows in a pipe and many other flow systems.

One step in the study of fluid dynamics systems is to define the important parameters in the problem. These parameters could be the Reynolds number, or any dimensionless combination of length, velocity, and time scales with fluid properties. The stability analysis involves pinpointing the critical value of these parameters for the transition.

The central question in stability analysis is: can a given flow field withstand a disturbance and still return to its original state? If so, it is stable; otherwise, that particular flow pattern is unstable to the imposed disturbance. If a flow is unstable to infinitesimal disturbances, then it cannot exist in nature even if it satisfies the conservation principles.

As an example, consider Reynolds' experiment with flow in a circular tube. A one-dimensional flow with parabolic velocity profile in the tube satisfies the mass, momentum, and energy conservation principles for $0<Re<\infty$. However, it is well known that in reality, this one-dimensional flow field ceases to exist for Re greater than a critical value[1*]. At this critical Reynolds number, there is a transition from the one-dimensional Poiseuille flow to a qualitatively different flow pattern. The mass, momentum, and energy conservation equations cannot predict this transition except through stability analysis. This involves examining the growth rate of all possible disturbances imposed on the base flow field as a function of the flow parameter, Re. The smallest value of the Reynolds number where a disturbance grows is the critical value for the transition. This is illustrated in the next section by a simple example.

A simple demonstration of relative stability is shown in Fig. I.2, where a ball is positioned in various states. Fig. I.2a presents an unconditionally stable system because the ball will return to its original state no matter how severely disturbed. In contrast, the state presented by Fig. I.2b is an unstable one since even an infinitesimal disturbance will take the ball

---

1* As Reynolds concluded from his experiments, and as later experiments have supported, the Poiseuille flow in a circular tube soon becomes unstable to finite amplitude disturbances. The critical Reynolds number for this instability is about 2000. Well-controlled laboratory experiments with extremely smooth-walled tubes have shown that the Poiseuille flow ceases to exist at a critical Reynolds number of about 40,000.

permanently away from its original state. This is also referred to as a *locally* or a *linearly* unstable system. A *neutrally* stable system is symbolized as a ball over a flat horizontal plane, as shown in Fig. I.2c, where the position remains fixed regardless of the disturbance. One should not confuse a neutrally stable state with *marginal* stability. In the latter case, the system loses stability at a neighboring value of the critical parameter.

Fig. I.2d illustrates a more complicated but physically important situation. The ball is in a stable state with regard to small amplitude disturbances but will destabilize and leave its original state when disturbed by a finite amplitude disturbance. This is an example of a *locally stable*, but *globally unstable* system.

In general the stability analysis can be divided into two categories, instability to (a) infinitesimal disturbances (local/linear), and (b) finite-amplitude disturbances (global/nonlinear). In this paper, we are mainly concerned with small disturbances, although globally unstable flows are also possible in coating systems [1].

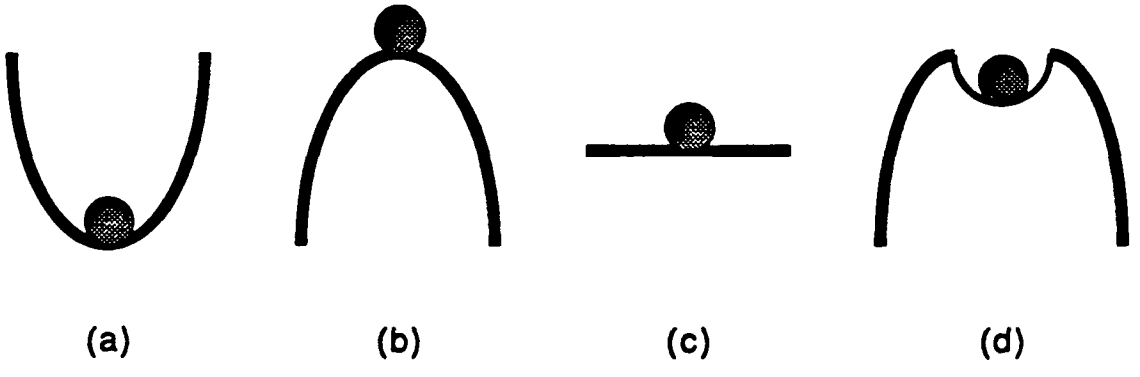

Figure I.2 Relative stability characteristics, (a) unconditionally stable; (b) unstable; (c) neutrally stable; and (d) locally stable but globally unstable.

The governing fluid dynamics equations are a set of coupled nonlinear partial differential systems which are well established. Closed form solutions to these equations are only available for simple ideal flows. Powerful numerical techniques, however, can be used to obtain solutions for the more complicated practical problems. A review of these techniques is provided by Kistler & Scriven (1983).

The general approach to analyzing the behavior of a flow to small disturbances is as follows: Let $\overline{U}$ represent the solution for the base state for which stability is under investigation. A small-amplitude disturbance, $\varepsilon\ u'$ (where $\varepsilon << 1$) is added to the base flow, $u = U + \varepsilon\ u'\ (\underset{\sim}{x}, t)$ and the resulting sum is substituted in the governing flow equations which are nonlinear in general. The terms that involve only the base state cancel identically and the resulting disturbance equation for u' is made linear by neglecting the higher order terms in ε. The critical Reynolds number where the disturbance u' starts to grow with time signals the onset of instability and transition of the base flow U. Let us illustrate this procedure with a simple example -- the break-up of an inviscid liquid jet in air.

I.1 INSTABILITY OF LIQUID JETS

For illustration purposes, in this section we review Rayleigh's (1879) stability analysis of an inviscid cylindrical liquid jet, much like a thin jet of water from a hose, and its break-up into drops. The steps involved in the linear stability analysis are typical and will be illustrated with this simple problem.

The equation governing the motion of an incompressible inviscid fluid is the Euler's equation, given by

$$\frac{\partial \underset{\sim}{u}}{\partial t} + \underset{\sim}{u} \bullet \nabla \underset{\sim}{u} = -\frac{1}{\rho} \nabla p \tag{I.1}$$

and the continuity equation

$$\nabla \bullet \underset{\sim}{u} = 0 \tag{I.2}$$

where $\underset{\sim}{u}$ is the velocity vector with components u_r, u_θ, and u_z in the r, θ, and z directions, respectively (Fig. I.3). The dependent variable $\underset{\sim}{u}$ and p are given by

$$\underset{\sim}{u} = U + \varepsilon \underset{\sim}{u}' \tag{I.3}$$

$$p = P + \varepsilon p' \tag{I.4}$$

where (U, P) correspond to the base flow, ε ($\underset{\sim}{u}'$, p') are the disturbances, and $\varepsilon << 1$. For convenience, we fix the coordinate system with the jet, so that the solution for the base flow can be written as

$$U = 0$$
$$P = P_a + \sigma/R$$

where P_a is the ambient pressure and R is the radius of the undisturbed circular jet. After the disturbance, the jet is no longer necessarily circular and in general its shape may vary

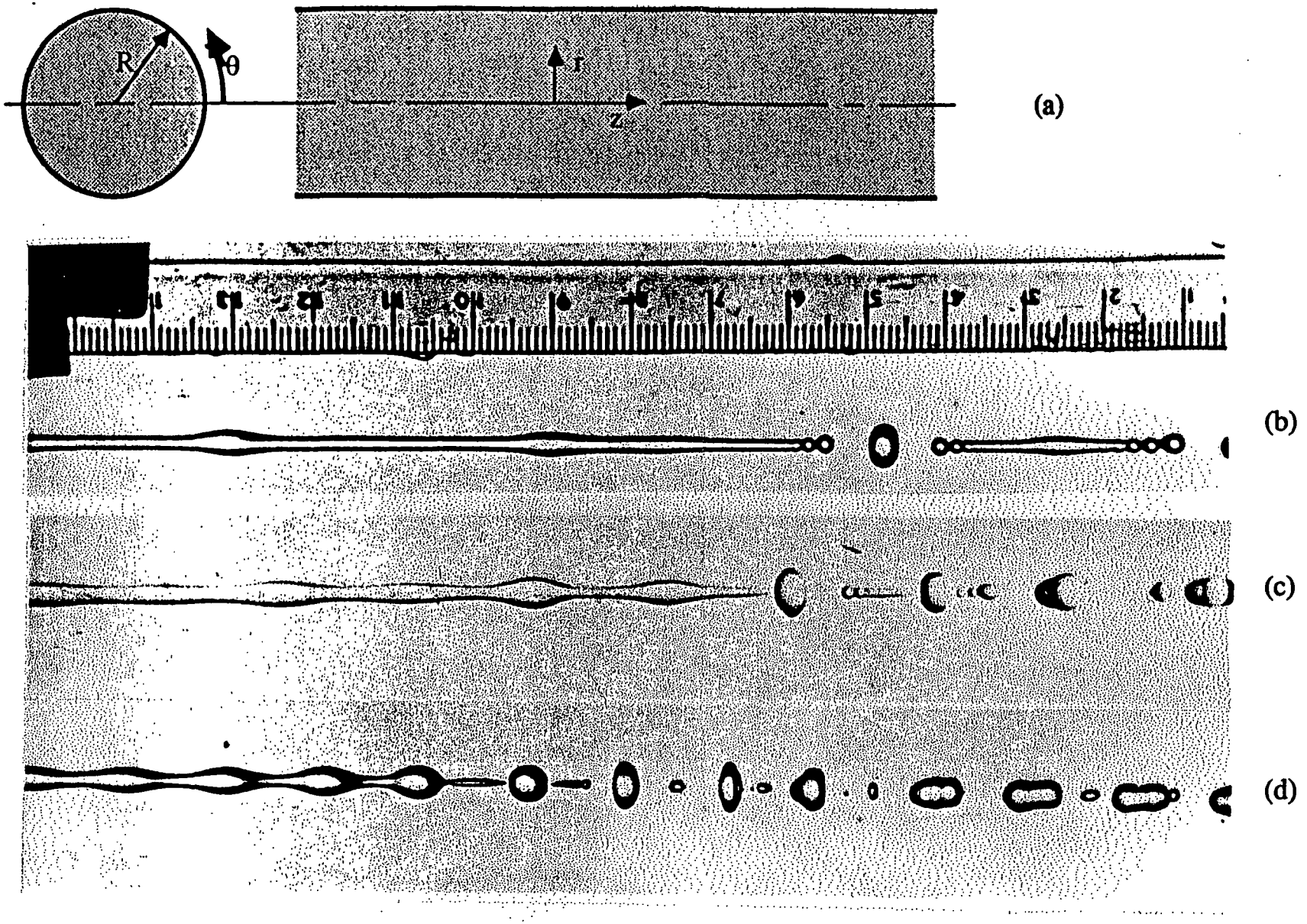

Figure 1.3 Break-up of a liquid jet, (a) schematic diagram illustrating the coordinate system; pictures show critical modes with wavelengths (b) 84R, (c) 25R, (d) 9.2R; the last being Rayleigh's prediction for the most likely destabilizing disturbance mode (from Rutland and Jameson, 1971).

slightly from a perfect cylinder, r = R, to an orbitary shape described as $r = \xi(\theta, z, t)$, where the disturbance function $\epsilon \xi' = \xi - R$. The dynamic and kinematic boundary conditions at the free surface of the jet ($r = \xi$) are given by

$$p = P_a + \sigma \nabla \bullet \underset{\sim}{n} \tag{I.5}$$

$$u_r = \frac{D\xi}{Dt} \tag{I.6}$$

where $\underset{\sim}{n}$ is the outward unit vector normal to the disturbed surface, $r = \xi$. By neglecting terms which contain $O(\epsilon^2)$ and higher, the disturbance equations and corresponding boundary conditions reduce to

$$\frac{\partial \underset{\sim}{u'}}{\partial t} = -\frac{1}{\rho} \nabla p' \tag{I.7}$$

$$\nabla \bullet u' = 0 \tag{I.8}$$

$$p' = \frac{\sigma}{R^2}\left(\xi' + \frac{\partial^2 \xi'}{\partial \theta^2} + R^2 \frac{\partial^2 \xi'}{\partial z^2} \right), \qquad r=R \tag{I.9}$$

$$u_r' = \frac{\partial \xi'}{\partial t}, \qquad r=R \tag{I.10}$$

Since the base flow is axially symmetric and the coefficients of the disturbance equations are functions of r alone, we can write the disturbance functions in normal modes as

$$(u', p', \xi') = (\hat{u}(r), \hat{p}(r), \hat{\xi}) e^{i\alpha z/R + st} \tag{I.11}$$

Where α is the wavenumber. Note that here we are considering only axisymmetric disturbances (no dependence on θ) since the jet is stable to all non-axisymmetric modes. Our objective is to evaluate the eigenvalue, s. If $s < 0$, then the jet is stable; otherwise it is unstable.

By taking the divergence of Eq. I.7 and substituting Eq. I.11 into the resulting Laplacian, we get

$$\frac{d^2\hat{p}}{dr^2} + \frac{1}{r}\frac{d\hat{p}}{dr} - \left(\frac{\alpha}{R}\right)^2 \hat{p} = 0 \ , \tag{I.12}$$

which is just the zero order modified Bessel equation. Considering that pressure should remain bounded as $r \rightarrow 0$, the solution is simply

$$\hat{p} = A\, I_o(\alpha r/R) \tag{I.13}$$

and from (I.7)

$$\underline{\hat{u}} = -\frac{A\alpha}{\rho s R}\left[i\, I_o(\alpha r/R)\ ,\ I_o'(\alpha r/R)\ ,\ o\right]. \tag{I.14}$$

The boundary conditions (I.9) and (I.10) give the relation for eigenvalue, s

$$s = \pm\left[\frac{\sigma\alpha}{\rho R^3}(1-\alpha^2)\frac{I_o'(\alpha)}{I_o(\alpha)}\right]^{1/2} . \tag{I.15}$$

Since $\frac{\sigma\alpha}{\rho R^3}\frac{I_o'(\alpha)}{I_o(\alpha)}$ is positive for any non-zero real value of α, the eigenvalue s becomes positive when $\alpha < 1$. In other words, the jet becomes unstable to disturbances with wavelengths, $\lambda = 2\pi R/\alpha$, which are greater than the circumference, $2\pi R$, of the jet. The eigenvalue s given by Eq. I.15 is plotted in Fig. I.4. The maximum growth rate corresponds to disturbance waves with wavelength $\lambda = 9R$. The idea that the dominant mode is likely to be the fastest growing mode was first suggested by Rayleigh (1879). This is not strictly true, however, since different modes within the range $o < \alpha < 1$ can

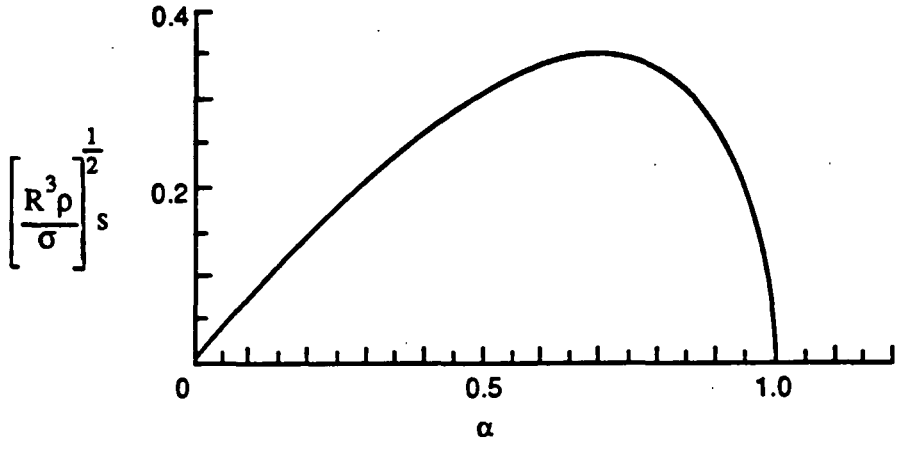

Figure I.4. Growth rates of a uniform jet with respect to unstable capillary modes.

become dominant (Fig. I.3), grow, and break the jet into droplets. The size of the droplets can be obtained from the radius of the jet and the wavelength of the most destabilizing disturbance mode.

I.2 INSTABILITY OF PARALLEL SHEAR FLOWS

Steady two-dimensional flows with parallel streamlines occur in many coating systems (a familiar example would be the flow under the blade in a blade coating device). Therefore, understanding the stability properties of this class of flows is important and necessary.

The stability properties of inviscid parallel flows are well established [16] and in general, the necessary conditions for instability are: a) the velocity profile has a point of inflection [22], and b) the absolute value of the vorticity be a maximum at the point of inflection [10]. Addition of viscosity could have a stabilizing or destabilizing effect. In general the critical Reynolds number for the growth of two-dimensional disturbances in a laminar parallel flow is lower than the critical Reynolds number for growth of three-dimensional disturbances [30].

Two simple but important parallel flows are the flows between two parallel solid planes, one driven by the motion of one plane relative to the other (plane Couette flow) and the other driven by a constant pressure gradient (plane Poiseuille flow, Fig. I.5). In a blade coating system, the flow under the blade in the nearly parallel gap is roughly a combination of the plane Couette and plane Poiseuille flows (Fig. I.5c).

Although the Navier-Stokes equations applied to these parallel flows reduce to linear systems and can be easily solved for the velocity profiles, solving the disturbance equations for stability analysis is not by any means trivial. In general, the disturbance equations for parallel flows reduce to a fourth-order linear homogeneous ordinary differential equation with complex coefficients [17,29]. For a given base flow and boundary conditions, this equation, which is referred to as the Orr-Sommerfeld equation, can then be solved for the neutral stability curves.

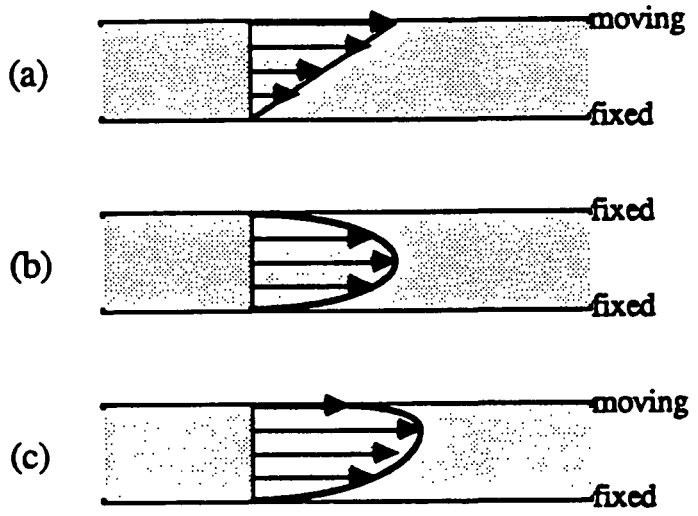

Figure I.5 Flow between parallel planes, (a) Couette; (b) Plane Poiseuille; and (c) Couette-Poiseuille flows.

Although the solutions for the velocity profiles shown in Fig. I.5 always satisfy the governing fluid mechanics conservation principles, the Orr-Sommerfeld equation shows that these parallel flows destabilize to infinitesimal disturbances at a finite critical Reynolds number. In the case of a plane Poiseuille flow, the most accurate value of the critical Reynolds number reported is $R_c = 5772.22$, which is obtained by Orszag (1971) using numerical expansions of the Orr-Sommerfeld equation in Chebyshev polynomials. Therefore, the velocity profile of Fig. I.5b can exist only in practice when $R < R_c$. Since the destabilizing disturbance structure is two-dimensional and symmetric with respect to the centerline, when R is slightly larger than R_c, a transition occurs to a second laminar flow which is also two-dimensional, steady state, and spatially periodic in the flow direction.

In a blade coating system, if the parallel streamlines under the blade destabilize, it is likely they will be replaced initially by a steady two-dimensional laminar flow with unparallel streamlines. Only then can there be transition to a three-dimensional state.

I.3 CENTRIFUGAL INSTABILITY OF ROTATING FLOWS

The first study of the instability of rotating flows was done by Rayleigh (1880) more than a century ago. Rayleigh's criterion for stability of a circulating inviscid fluid simply states that

$$\phi(r) \equiv \frac{1}{r^3} \frac{d}{dr} (r^2 \Omega)^2 > 0$$

everywhere in the field of flow. Here $\Phi(r)$ is the Rayleigh discriminant and the angular velocity of the fluid, $\Omega(r)$ is an arbitrary function of the position r from the axis of rotation. This general criterion is limited to axisymmetric disturbances. The transition in circulating flows is mainly based on centrifugal instability. To illustrate, we will review Rayleigh's physical discussion of centrifugal instability for an inviscid fluid.

The radial momentum balance for an axisymmetric flow states

$$\frac{D}{Dt}(ru_\theta) = 0$$

where $\frac{D}{Dt}$ is a material (substantial) derivative and u_θ (= r Ω) is the angular component of velocity. This equation simply states that the angular momentum of a fluid element, ru_θ, is constant. The centrifugal force density in the radial direction is

$\rho \frac{H^2}{r^3}$, and the kinetic energy is $\frac{1}{2} \rho \frac{H^2}{r^2}$.

Now consider fluid elements 1 and 2 rotating around the axis of rotation with an angular velocity at arbitrary positions $r = r_1$, and $r = r_2$, respectively. Let us assume that the fluid elements have an equal volume, δV. Then the total kinetic energy of the elements due to azimuthal motion is given by

$$KE_b = \frac{1}{2} \rho \left(\frac{H_1^2}{r_1^2} + \frac{H_2^2}{r_2^2} \right) \delta V.$$

If we interchange fluid elements 1 and 2 such that element 1 is rotating with radius r_2 and fluid element 2 with radius r_1, then the total kinetic energy of the system will be equal to

$$KE_a = \frac{1}{2} \rho \left(\frac{H_1^2}{r_2^2} + \frac{H_2^2}{r_1^2} \right) \delta V.$$

The difference in the kinetic energy from states b to a is given by

$$KE_a - KE_b = \frac{1}{2} \rho \left(H_2^2 - H_1^2 \right) \left(\frac{1}{r_1^2} - \frac{1}{r_2^2} \right) \delta V.$$

If $r_2 > r_1$ and $H_2 < H_1$ (i.e., if $\frac{dH}{dr} < 0$, a violation of Rayleigh's criterion for stability), the net change in kinetic energy due to the interchange of fluid elements is negative (state a

requires less kinetic energy) and therefore, the rotating flow is unstable. This result is of course limited to axisymmetric disturbances. The stability properties with respect to more general disturbances are treated by Synge (1938).

In general, viscosity has a stabilizing effect in a rotating flow. Therefore, if a basic flow is stable according to Rayleigh's criterion then it must remain stable as viscosity is introduced into the system. On the other hand, if a system does not satisfy Rayleigh's criterion for stability, then adding viscosity may or may not have a stabilizing effect.

The Taylor-Couette Problem

Perhaps the most popular example of a system which exhibits centrifugal instability is the Taylor-Couette cell where fluid is contained between two concentric rotating cylinders (Fig. I.6). This system was analyzed by Taylor (1923) who obtained the curve of marginal stability in the plane of the angular velocity of the inner and outer cylinders. The two-dimensional basic flow destabilizes at a critical Reynolds number and gives rise to donut-shaped vortices, sometimes referred to as Taylor vortices (Fig. I.6b). The Reynolds number for this problem can be defined as $R_T = R\,(\frac{d}{R_1})^{1/2}$ where $R=R_1\Omega d/\nu$. Here d is the gap between the two cylinders, and R_1 and Ω are the radius and the angular velocity of the inner cylinder, respectively. The critical Reynolds number for the onset of Taylor vortices in an ideal system is about 41.3. As the Reynolds number is increased, a second transition replaces the steady state flow with a time-periodic state (Fig. I.6c). For an infinitely long cylinder, these vortices are perfectly uniform and periodic in the axial direction. A finite length cylinder, however, introduces some imperfections due to the end boundaries.

Burkhalter and Koschmieder (1973) showed that in a long circular Couette cell, resting end walls fixed with the resting outer cylinder produce a sink at the boundary, that is, the fluid moves inward near the boundaries. On the other hand, when end walls rotate with the inner cylinder, then a source generates at the end boundaries. Also, multiple stable states are shown to exist in finite length systems.

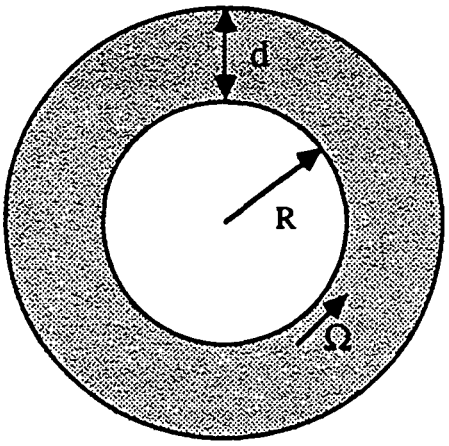

(a)

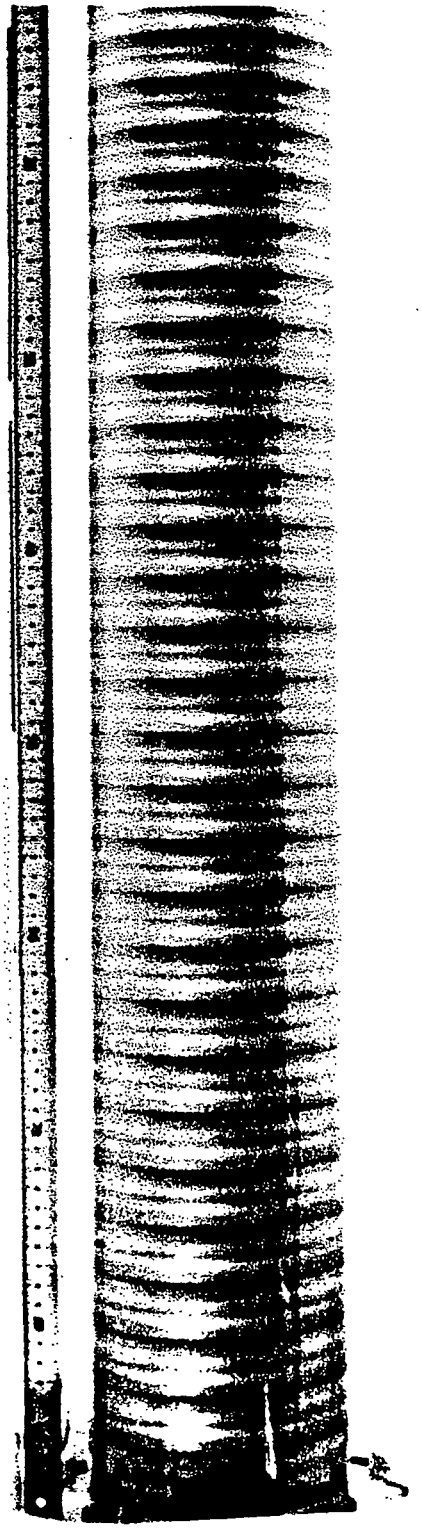

(b)

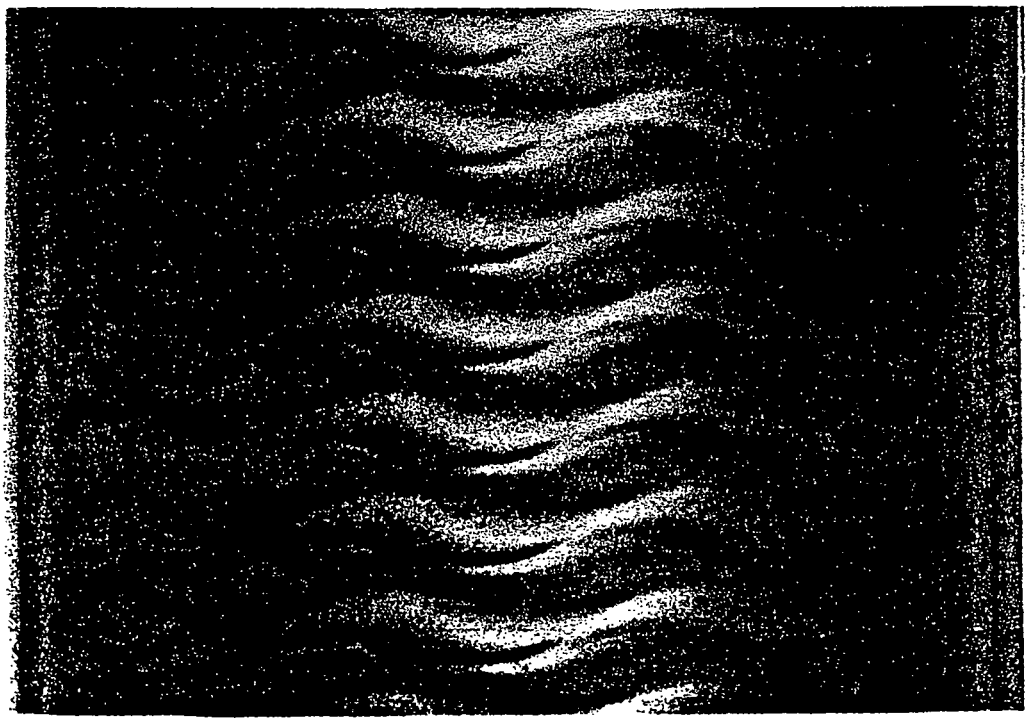

(c)

Figure I.6 Flow between concentric rotating cylinders; (a) schematic of cross section; (b) Steady Taylor vortices; (time-periodic state (from Koschmieder, 1979).

A closely related case is the Taylor-Dean problem where, in addition to the rotation of the cylinder, an azimuthal pressure gradient is also present. This problem was originally studied by Brewster and Nissan (1958) and Brewster, Grosberg, and Nissan (1959). Similar to the Taylor problem, the instability is made evident by the appearance of toroidal vortices. Raney and Chang (1971) showed that the system is also unstable to oscillatory disturbances.

The Dean Problem

A pressure driven flow in a curved channel (Fig. I.7) can also exhibit centrifugal instability. The first study of this problem is by Dean (1928) who considered the flow in a narrow channel formed by two coaxial cylinders. For a constant pressure gradient acting in the azimuthal direction and with the narrow-gap approximation, the velocity distribution is given by the parabolic form of the plane Poiseuille flow,

$$v(r) = \left\{ 1.5 - \frac{6}{d^2}\left[r - \frac{1}{2}(R_1 - R_2) \right]^2 \right\} V_o$$

where $d = R_2 - R_1$ and V_0 is the mean velocity across the channel. The Reynolds number for this problem (sometimes referred to as the *Dean number*) is given by $R_D = R \left(\frac{d}{R_1} \right)^{1/2}$ where $R = V_0 d / \nu$. The flow represented by the velocity profile v(r) can destabilize by two entirely different mechanisms. In addition to the centrifugal instability which necessarily includes three-dimensional disturbances, this flow, an approximately parallel shear layer, can also destabilize to two-dimensional disturbances. The question is, when would each instability mechanism be the dominant one? To answer this question let us consider the critical parameters for the onset of each instability.

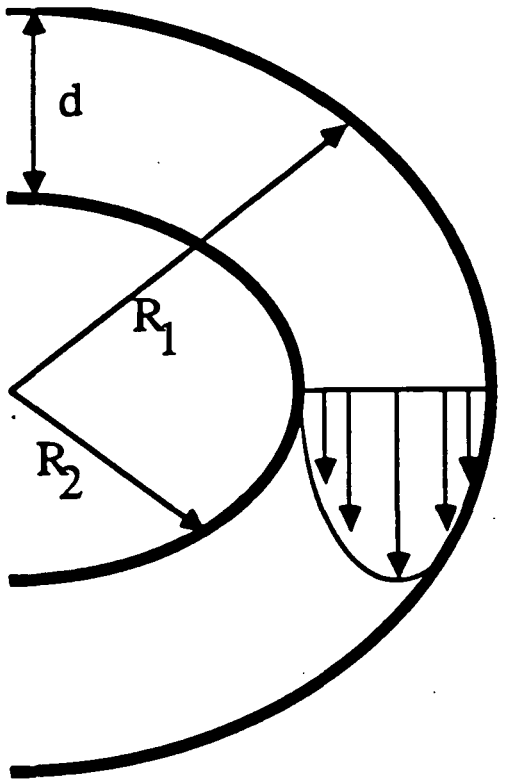

Figure I.7 Pressure driven flow in a curved channel.

The critical value of the Dean number, R_D, signaling the onset of three-dimensional disturbances, is about 35.9. On the other hand, the critical Reynolds number, R_C, for the instability of plane Poiseuille flow to two-dimensional disturbances is about 5772x4/3. Therefore, when $R_C(d/R_1)^{1/2} < 35.9$ (i.e., when $\frac{d}{R_1} < 2.17\text{x}10^{-5}$) the first supercritical state of the flow remains two-dimensional, otherwise three-dimensional vortices appear due to centrifugal instability.

Therefore, for a pressure driven fluid layer in a curved channel to behave as a parallel shear flow, the ratio for gap to radius of curvature has to be less than about $2\text{x}10^{-5}$. This rather general conclusion will be useful as a guide in various coating flows which may exhibit potential for both kinds of instability mechanisms.

Görtler Instability In Boundary Layer Flows

A third classic problem which exhibits centrifugal instability is the formation of a thin viscous boundary layer over a concave wall. By definition, a boundary layer over a solid surface is a thin layer across which the fluid velocity increases from zero (no-slip) at the wall to the free-stream velocity. Viscous effects are then important only inside the boundary layer. This condition appears only when the Reynolds number based on the free stream velocity is sufficiently large. Boundary layer flow over a concave solid surface is prone to centrifugal instability which results in the formation of counter rotating toroidal vortices with axis of rotation parallel to the direction of the base flow (Fig. I.8). These vortices are referred to as Görtler vortices. Görtler's (1942) analysis assumes that the boundary layer thickness is much smaller than the radius of curvature of the wall and also that the base flow is nearly parallel to the wall, therefore, centrifugal effects are important only in the boundary layer region.

It is then easy to show that the Rayleigh discriminant in this problem is proportional to $-V\frac{dV}{dy'}$ where $y' = \frac{y}{\delta}$, δ is the boundary layer thickness, and the fluid velocity, V, increases inside the layer from y=0 at the solid surface to y=δ at the free stream. The Rayleigh discriminant is therefore always negative, which indicates that the flow can become unstable in the boundary layer.

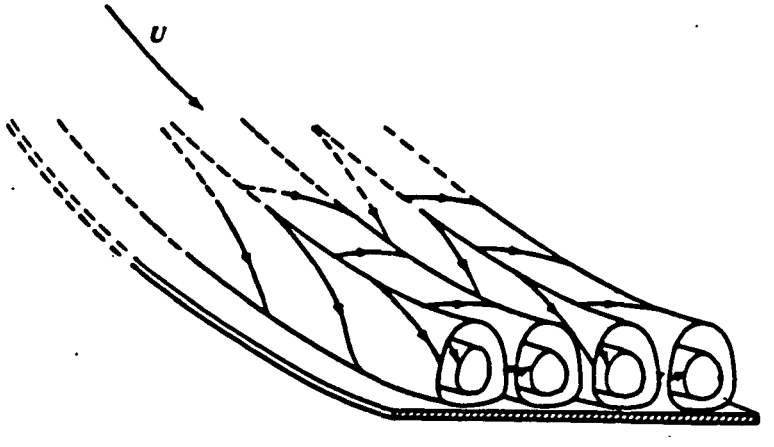

Figure I.8 Görtler Vortices in a boundary layer along a concave wall.

The next section mainly contains examples of flow instability in coating systems along with more classical flow instability problems. Also, some generalizations of the behavior of dynamical systems are discussed in Section III.

II. EXAMPLES OF FLOW INSTABILITY IN COATING SYSTEMS

In this section, examples of flow instability in coating systems will be discussed along with some relevant classical problems. By comparing practical instability problems in coating systems with relevant prototype problems, we can understand the origin and mechanism of the instabilities.

II.1 FLOW INSTABILITY IN BLADE COATING

Blade coating, the most popular mode for surface application of paper and board, is one of the most complex and interesting hydrodynamic devices. The fluid (coating color or size) is forced from one extreme to another and the fluid particles experience changes in the shear rate from almost zero upstream of the blade to nearly 10^6 (1/sec) under the blade in about 10^{-2} seconds. Regions with enormous pressure gradients are adjacent to nearly constant pressure areas (pressure-plateau), and orders of magnitude differences exist in the velocity gradients.

In addition to these complexities, one could hardly design a problem with more complex boundaries. The blade is flexible, the web is flexible and permeable, and there are free-surfaces with static and dynamic contact lines. The expectations for an ideal coating device are also extreme, i.e., the flow needs to remain steady and two-dimensional (no velocity component and momentum transfer in the cross machine direction) at high machine speeds for ideal operating conditions.

Every type of instability mechanism mentioned in section I and beyond can destroy this "ideal" flow and result in unsteady or three-dimensional coating states with often intolerable consequences. The extreme flow conditions, complex fluid properties, irregular flow boundaries, and high expectations create new challenges which require advanced technological and scientific approaches. Combining results from carefully designed

laboratory experiments with the well-known principles of dynamical systems (next section) will provide useful information for the design of improved systems.

A second necessary and complementary approach is computer-aided experiments where the governing fluid flow equations are solved accurately using robust computational techniques. The governing fluid flow equations are well-established and their solutions can accurately simulate the physical situation -- accuracy being the key word. This approach has proved to be quite useful for example in the stability analysis of slide coating flows [6].

Computational analysis of blade coating, because of its extreme nature and complex boundaries, is a difficult and time-consuming (evolutionary) task. The benefits, however, are enormous, since in contrast to experiments where a limited amount of information can be extracted, an accurate or "exact" numerical solution of the governing equations of a fluid flow process provides complete information for every point in the domain. An example is the finite-element simulation of blade coating by Pranckh and Scriven (1988) which is the most detailed analysis of blade coating currently available. Although only two-dimensional flow equations are solved in this simulation, the quantitative results also shed light on the relative magnitude of forces and subsequently the hydrodynamic instability properties of the two-dimensional flow with respect to three-dimensional disturbances. This provides the basis for the discussions in this section.

Consider the flow in a blade coating system with a roll applicator (Fig. II.1). Various sections of the flow field exhibit unique characteristics. Here, the web is moving from left to right carrying a thick layer of fluid with it. The fluid in this layer (region 1) moves like a solid body and experiences almost zero shear. As this layer approaches the blade it bifurcates into roughly three streams. Stream A, adjacent to the web, continues into the nip of the blade (region 6) and experiences an enormous increase in shear rate. Layer B, the middle stream, falls just below the separation line (region 11), turns downward and forms two boundary layers, one on the flat surface of the blade (region 12) and a second next to the concave region of layer C. The free-surface stream (layer C) reflects down the blade under negligible viscous forces (irrotational flow).

In an incompressible fluid, a disturbance at one section propagates instantaneously throughout the media. Therefore, if three-dimensional disturbances grow upstream of the

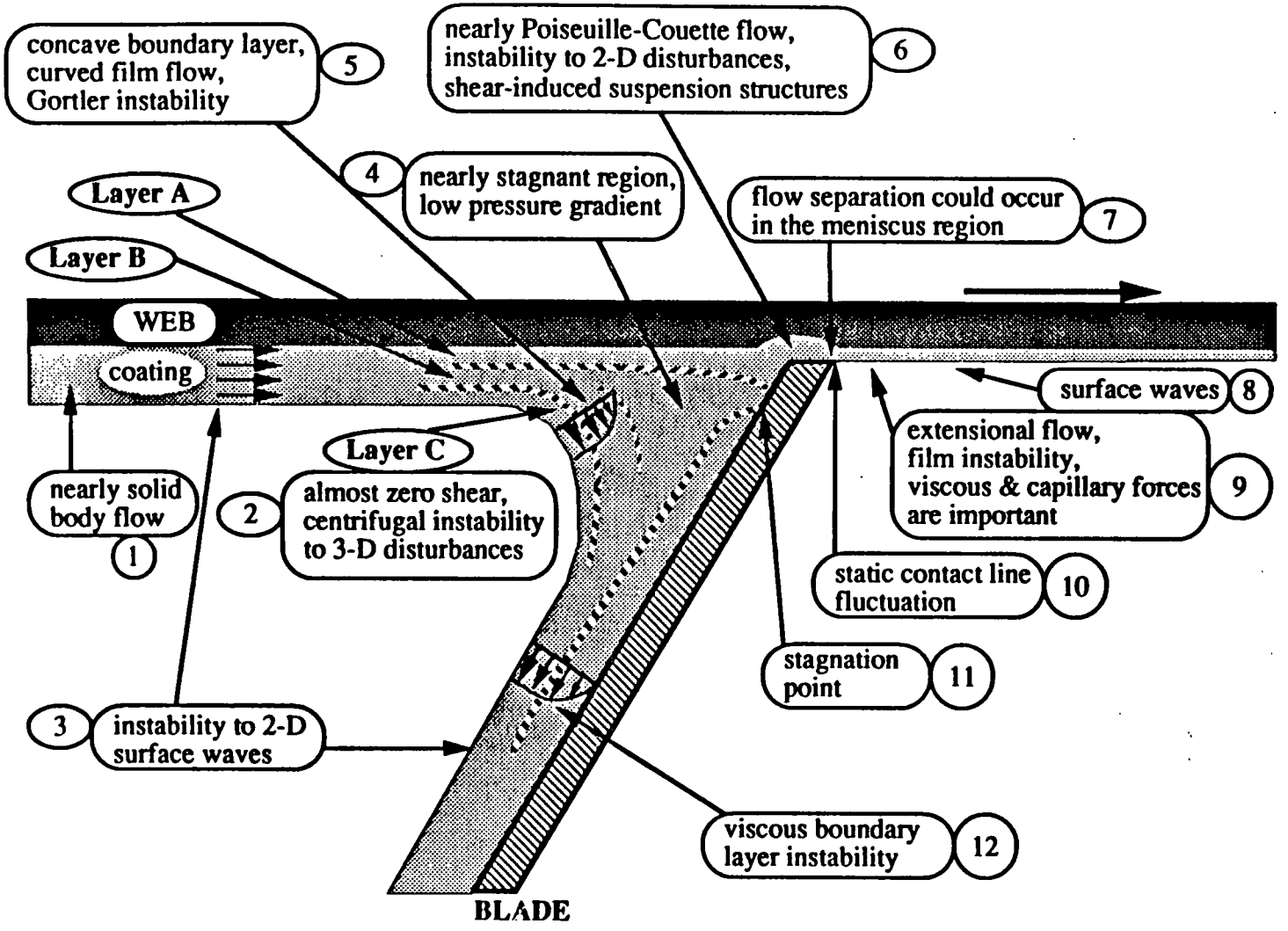

Figure II.1 Some stability characteristics of flow in blade coating with a roll applicator (see Pranckh and Scriven, 1988, for quantitative information).

blade, their effects will propagate through the blade tip and may result in coat weight nonuniformities (streaks, ...). Let us then casually investigate the stability properties of the three layers mentioned above.

Layer A enters a high-shear region under the blade and follows a nearly Poiseuille-Couette velocity distribution [19]. Following Squire's theorem the first instability will be due to a two-dimensional disturbance mode in the plane of the base fluid (section I.2). Further downstream in the meniscus region, however, other mechanisms such as visco-capillary instabilities become important.

The irrotational stream (layer C) is under a centrifugal force and could become unstable to three-dimensional disturbances. According to Rayleigh's criterion (section I.3), if the radial gradient of the magnitude of the angular momentum becomes negative, then the flow could become unstable. Let us assume that the curved section of this layer is circular where $r = R_1$ and $r = R_2$ define its inner and outer boundaries, respectively. Also, let u_θ, the azimuthal component of velocity, be a function of r alone and let other components of the velocity vector be negligible. The Rayleigh's criterion for stability reduces to

$$\frac{r}{u_\theta}\frac{du_\theta}{dr} > -1.$$

This presents an approximation for the stability criterion of layer C. A more accurate stability analysis can be obtained by actually calculating Rayleigh's discriminant along the streamlines given by Pranckh and Scriven (1988).

Between layers B and C in the curved section of the stream (region 12), the velocity rapidly decreases to zero forming a concave boundary layer susceptible to Görtler-Taylor type instabilities. This boundary layer, in conjunction with layer C, roughly forms a free-surface curved film. This flow is similar to a free-surface film flow down a concave wall which could become unstable to Görtler-type vortices in the concave region [27]. The critical Reynolds number, $Re \equiv \frac{U_0\delta}{\nu}\left(\frac{\delta}{R}\right)^{1/2}$, (based on the radius of curvature, R, film thickness, δ, and the average film velocity, U_0) for onset of Görtler-type vortices for the case of a film falling under gravity alone is reported [27] to be about 16.1 which is close to

the value of 15.8 for the onset of Görtler instability in a boundary-layer over a concave wall.

A blade coating system with puddle or short-dwell applicators has somewhat different stability properties compared to the system considered above. In addition to the local instability discussed above, the *apparent two-dimensional* flow in the pond of these systems can be globally unstable. In fact, the flow of Newtonian fluids in a cavity simulating the pond of a short-dwell coater is shown to have multiple stable steady states [1].

II.2 CENTRIFUGAL INSTABILITY IN THE POND OF PUDDLE COATERS, SHORT-DWELL COATERS, AND SIZE PRESSES

Puddle and short-dwell coaters, along with size presses, are used extensively in the industry for surface applications. A description of these systems can be found in the review article by Eklund (1989).

All of these systems share a common hydrodynamic feature-- apparent two-dimensional rotating vortices (Figure II.2) which are prone to instability and transition to three-dimensional patterns. As stated above, flows with curved streamlines can destabilize to three-dimensional disturbances. It is this instability that replaces the ideal two-dimensional flow (no velocity components in CD) with the troublesome three-dimensional flow patterns in many coating systems. A three-dimensional flow pattern in the pond contains velocity components in the cross machine direction which often result directly or indirectly in coat weight nonuniformities in CD.

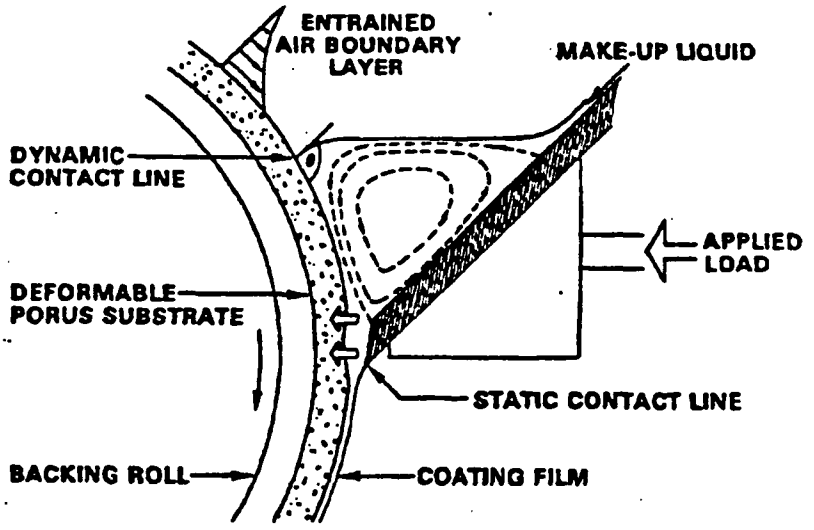

(a)

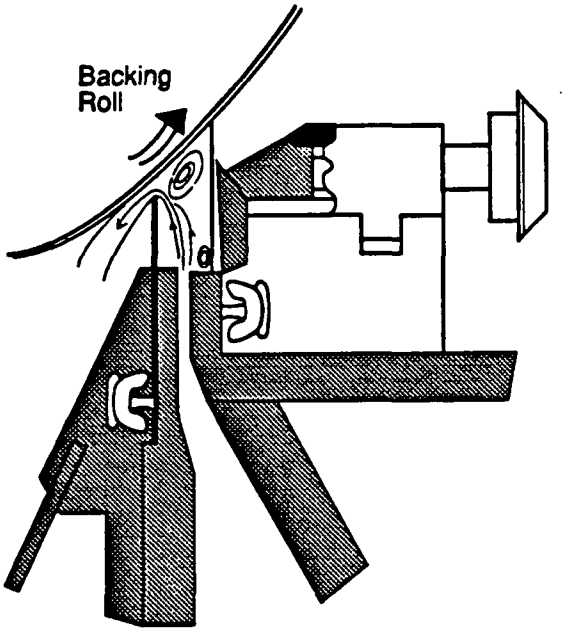

(b)

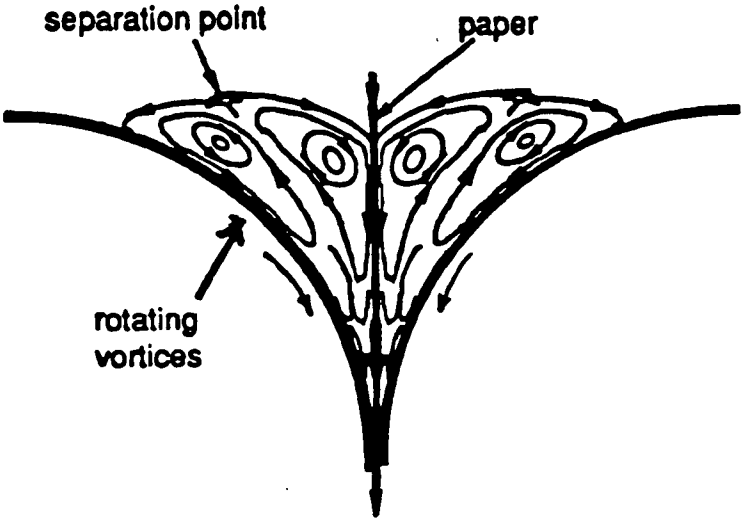

(c)

Figure II.2 Schematic of (a) experimental puddle coater; (b) short-dwell coater; and (c) size press.

The fact that three-dimensional disturbances in the pond upstream of the blade can lead to "streaking" defects in the coating film was reported first by Higgins (1981) in the case of a puddle coater. Higgins showed that a steady three-dimensional pattern (Fig. II.3) can develop in the pond upstream of the blade as a result of instability of the base state. Even more complex three-dimensional patterns can develop in the pond of short-dwell coaters. Fig. II.4b is the picture of one of the multiple steady three-dimensional patterns that can replace the apparent two-dimensional primary and secondary rolls (Fig. II.4a) in a driven cavity simulating the pond of a short-dwell coater [1].

It would be interesting to examine these multiple states and obtain the bifurcation diagram (see the next section) for the flow structures. If the three-dimensional states represent isolated solutions of the governing equations, then standard branch tracing techniques may not be sufficient to completely map the solution structure.

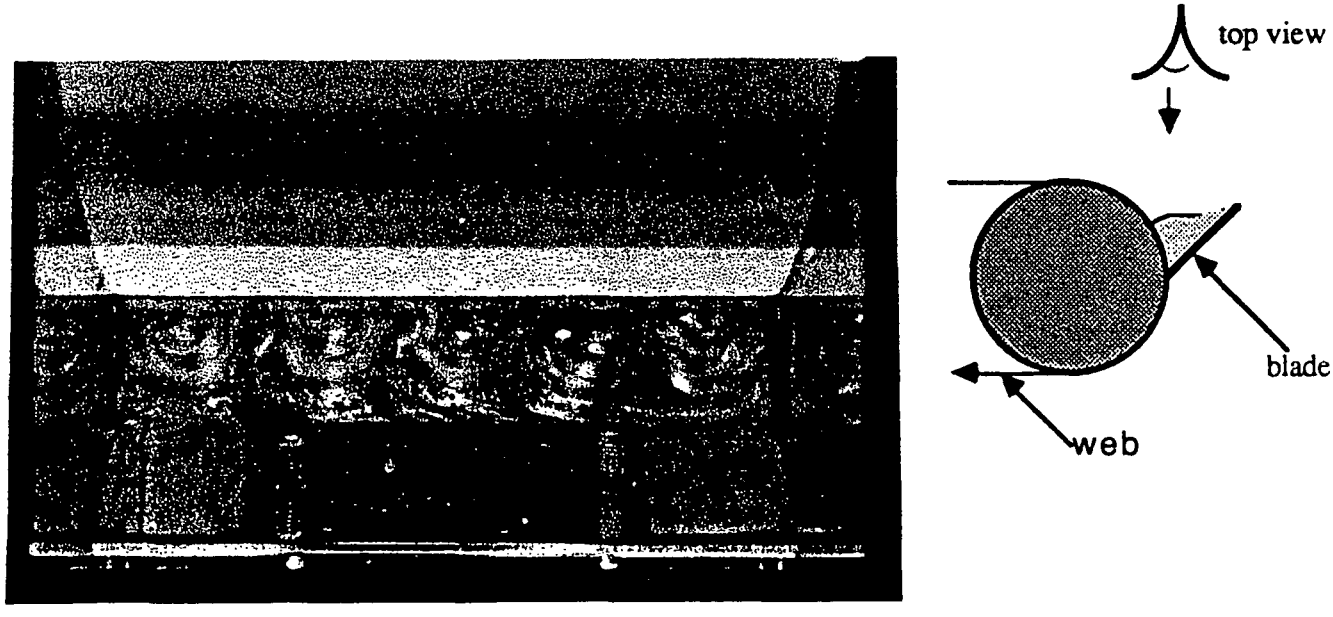

Figure II.3 Top view of the three-dimensional patterns in the pond of a puddle coater. The web moves down from top of the picture (see Fig. II2a for a schematic) at 500 ft/min (from Higgins, 1981).

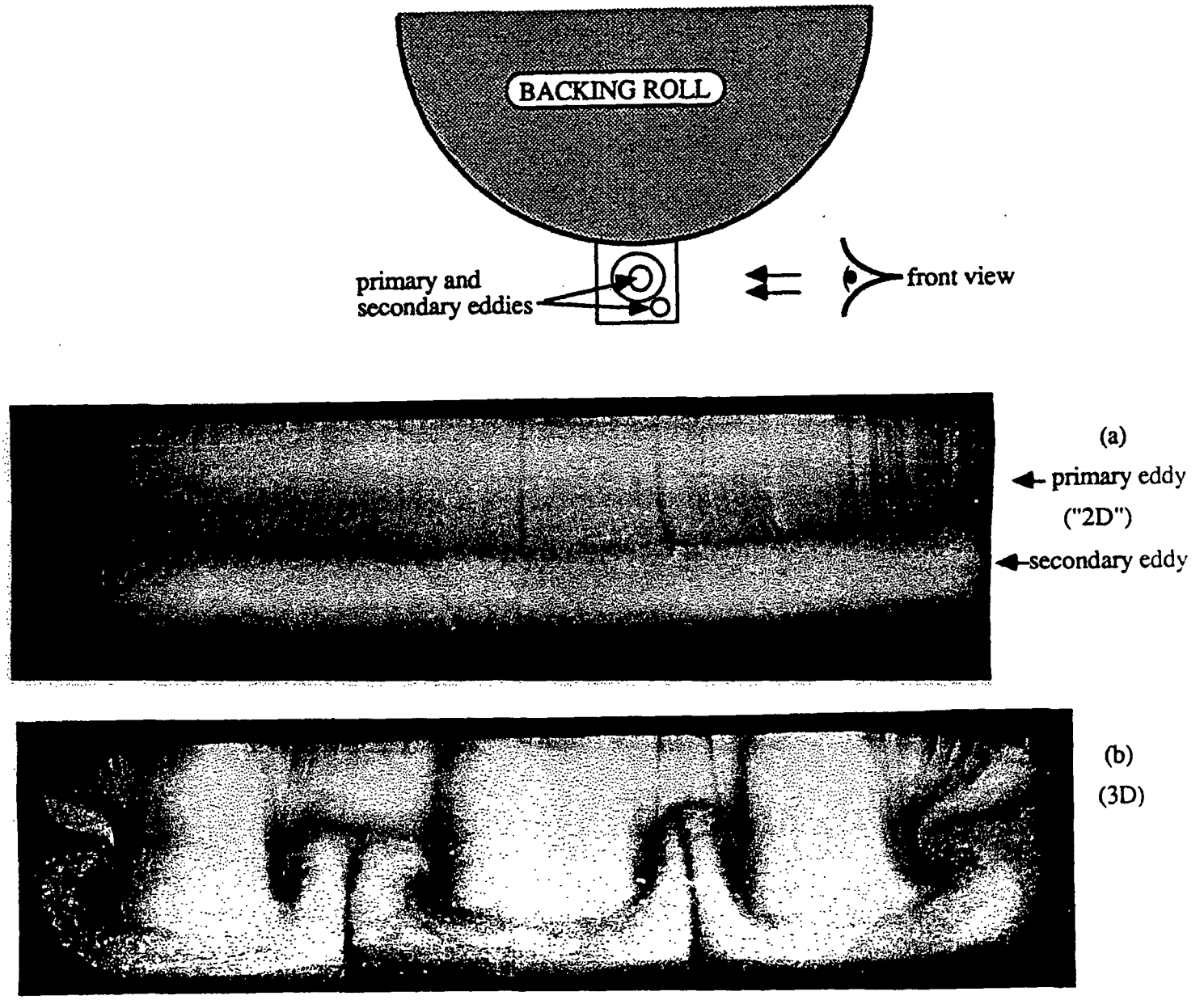

Figure II.4 Illustration of multiple steady states in the pond of a short dwell coater; (a) steady state which appears almost two dimensional ("2D"); (b) a second steady state with complex three-dimensional patterns which can replace the "2D" state at identical operating conditions. The pictures are the front view of flow in a rectangular cavity simulating the pond of a short dwell coater (from Aidun and Triantafillopoulos, 1990).

For linear instability, the disturbance structure could be steady or time-periodic which results in a steady or time-periodic three-dimensional flow. By simply rescaling and adding the destabilizing disturbance to the two-dimensional base flow, we can closely approximate the three-dimensional flow pattern near the point of onset. In the case of transition from steady to time-periodic flow (a Hopf bifurcation) in a different problem, this technique has proved to be quite effective and useful in understanding and explaining the instability mechanism [31].

Little is known about the flow instability of non-Newtonian fluids and suspensions in these surface application systems. A significant gap currently exists in this area. How can the current surface application technologies be improved and more advanced systems be developed in a rational and informative (cost-effective) manner without a fundamental understanding of these issues?

The classical flow problems reviewed in the previous section show that two-dimensional rotating flows can readily be replaced by three-dimensional flow patterns due to centrifugal instability. Size presses, puddle coaters, and short-dwell coaters are the most vivid examples of processes which include apparent two-dimensional rotating fluid vortices that are vulnerable to centrifugal instabilities. Continuing work on short-dwell coaters has shown a variety of interesting and unexpected results in terms of local and global stability properties. Possible instability mechanisms which can result in intolerable operating conditions in this system are outlined in Fig. II.5. The non-Newtonian effects have dramatic influence on the stability properties of recirculating flows and should be considered in future studies.

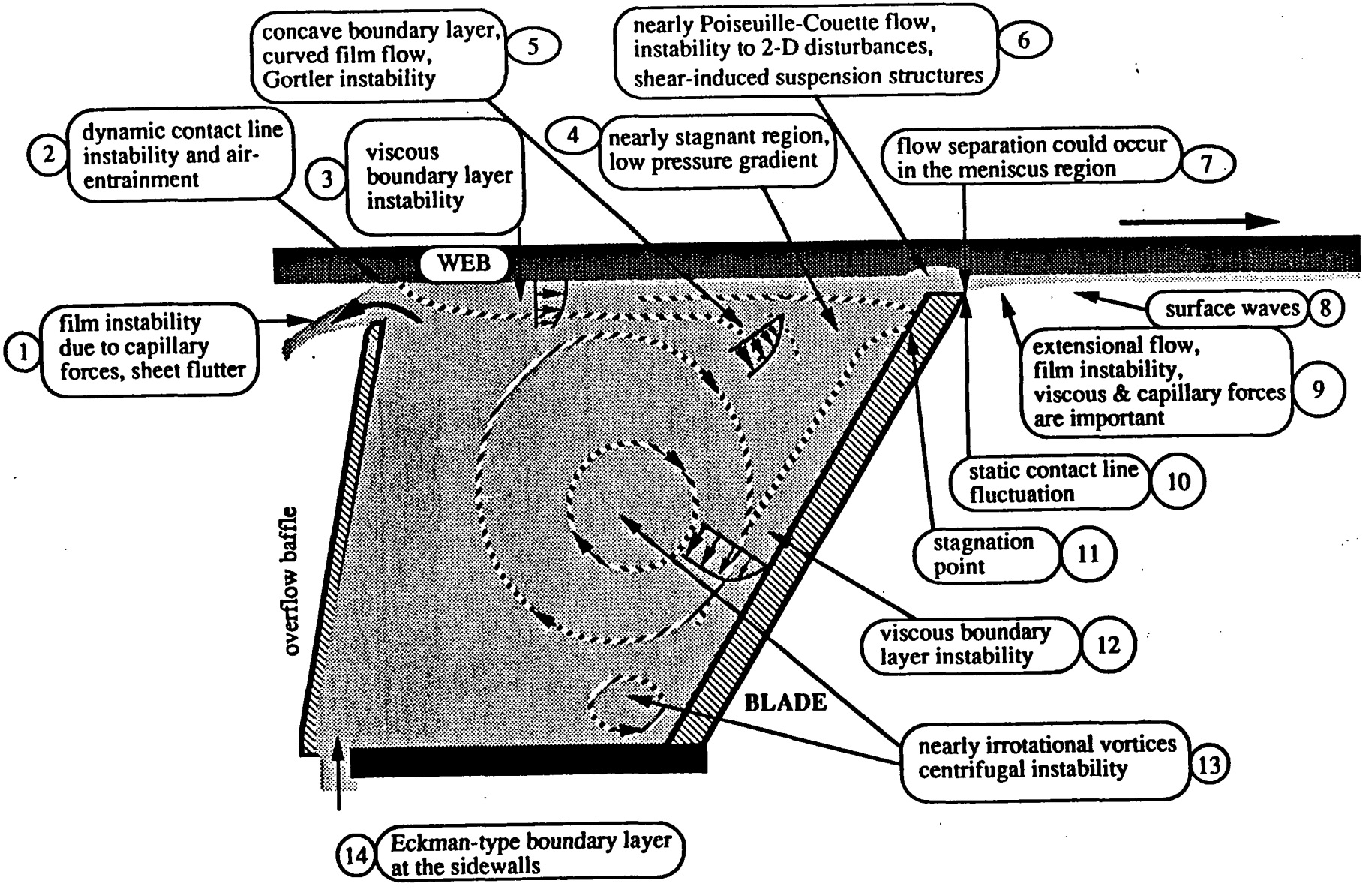

Figure II.5 Some stability characteristics of flow in blade coating with a short dwell time applicator.

II.3 RIBBING LINES IN FORWARD ROLL COATING

Ribbing instability in roll coating is a well known phenomenon and has been extensively studied. For a detailed discussion, see the review article by Ruschak (1985). A meniscus forms in the diverging section of the nip, as shown in Fig. II.6. The ideal condition is achieved when a steady two-dimensional flow field is maintained, that is, when there is no flow in the cross-machine direction. However, this two-dimensional flow destabilizes and gives rise to a three-dimensional flow pattern. It turns out that in this transition the flow becomes spatially periodic in the cross machine direction, and therefore, the free surface becomes ribbed and uneven (Fig. II.7). This usually results in unacceptable operating conditions.

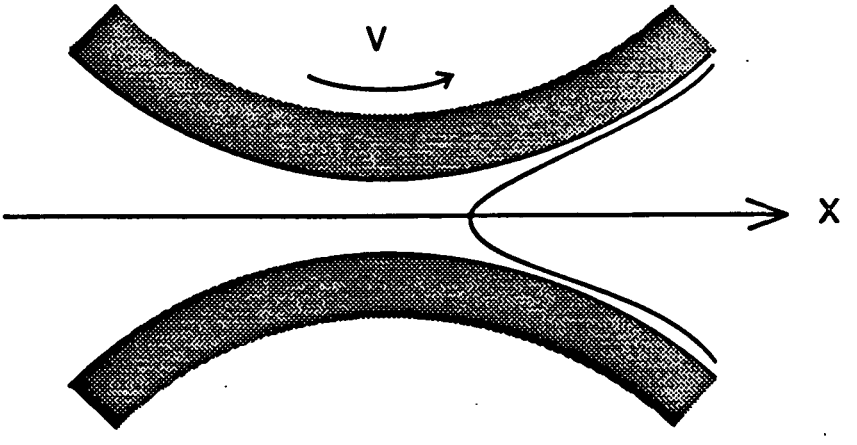

Figure II.6 Forward roll coating.

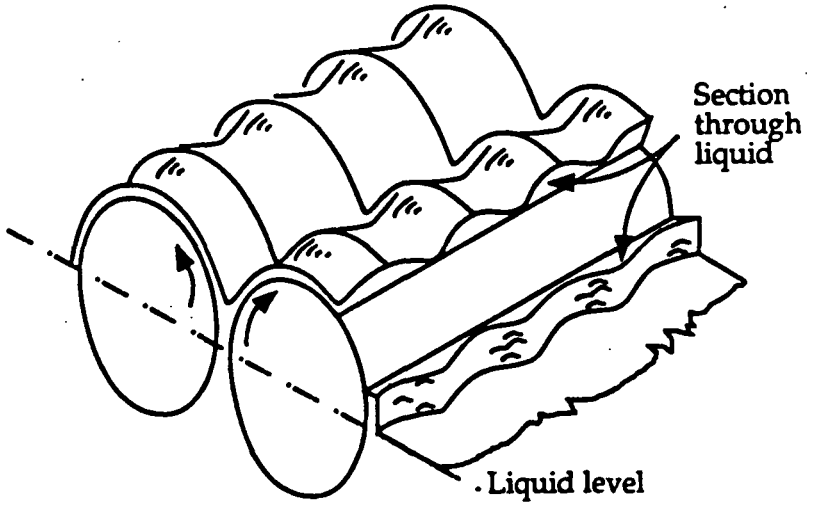

Figure II.7 Schematic of ribbing lines in forward roll coating.

The important parameter in this problem is the Capillary number, Ca, which is defined as $\mu V/\sigma$, where μ and σ are the viscosity and surface tension of the fluid, respectively, and V is the roll speed. For rolls with equal size and speed, the meniscus forms close to the center of the nip for a sufficiently large capillary number. This flow becomes unstable and ribbing lines appear when the capillary number exceeds a critical value. In the limit, this could be approximated as a meniscus forming between two nearly parallel planes moving with equal speed, V, as shown in Fig. II.8. The following question remains: What is the physical reason for the instability? In other words, why does the two-dimensional flow cease to exist beyond a critical capillary number?

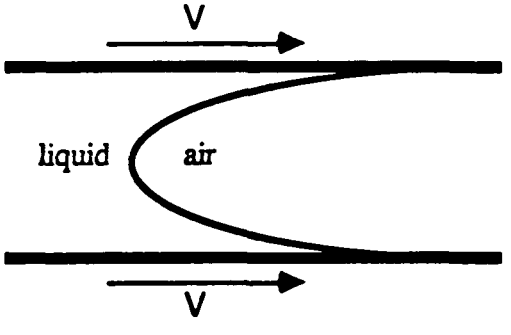

Figure II.8 A meniscus formed between two parallel solid surfaces.

The answer can be obtained from the classical instability analysis of Saffman and Taylor (1958), who consider the stability of air/liquid interface between two closely spaced parallel solid surfaces (Fig. II.9). Here fluid 2 is displacing fluid 1 through a sharp interface. Initially, the interface is assumed to be a straight line (Fig. II.9a) moving upward with velocity, V.

Using standard linear stability analysis (reviewed in the previous section) Saffman and Taylor showed that the interface becomes unstable to infinitesimal disturbances if

$\left(\frac{\mu_2}{k_2} - \frac{\mu_1}{k_1}\right)V + (\rho_2 - \rho_1)g < 0$, where k and ρ are permeability of the medium to the fluid, and the fluid density. Subscripts 1 and 2 refer to the upper and lower fluids, respectively.

In many situations, such as some coating flows, the acceleration due to gravity, g, may not be important. If we choose fluid 1 to be liquid and fluid 2 air, and fix the frame of reference relative to the meniscus, then Fig. II.9b represents an approximation of the forward roll coating problem, since for sufficiently large capillary numbers, the coating meniscus is near the nip where the roller surfaces are nearly parallel.

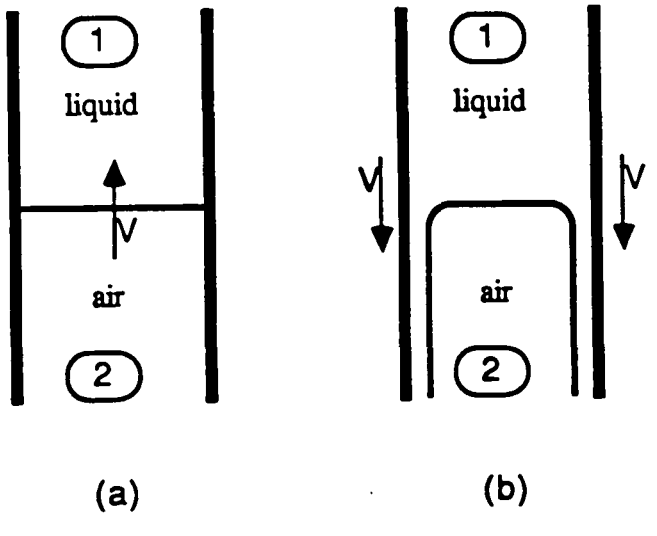

Figure II.9 Liquid displacing air between closely spaced parallel solid surfaces.

The linear stability analysis of Saffman and Taylor shows that if the pressure gradient, $\frac{dP}{dX}$, in the liquid adjacent to the meniscus in Fig. II.9 is positive, then the flow is unstable and ribbing lines appear. Using matched asymptotic expansion, Ruschak (1982) showed that the pressure gradient in this situation is always positive and the flow is therefore unstable.

Here the instability mechanism is pressure driven [18] and can be explained in the following way. Consider two neighboring points, A and B, on an undisturbed meniscus (Fig. II.10a) with a positive pressure gradient in the machine direction. Now let a small disturbance pull the surface by a small amount from point B to point B'. The pressure profile remains about the same but shifts upstream by a small length BB'. This disturbance creates a pressure gradient in CD. Since the pressure at the undisturbed neighboring points, such as point A, is now lower than pressure at B', this forces flow from disturbed points toward the undisturbed regions and reinforces the disturbance causing a positive growth rate. The disturbance structure with the most destabilizing wave length will grow first.

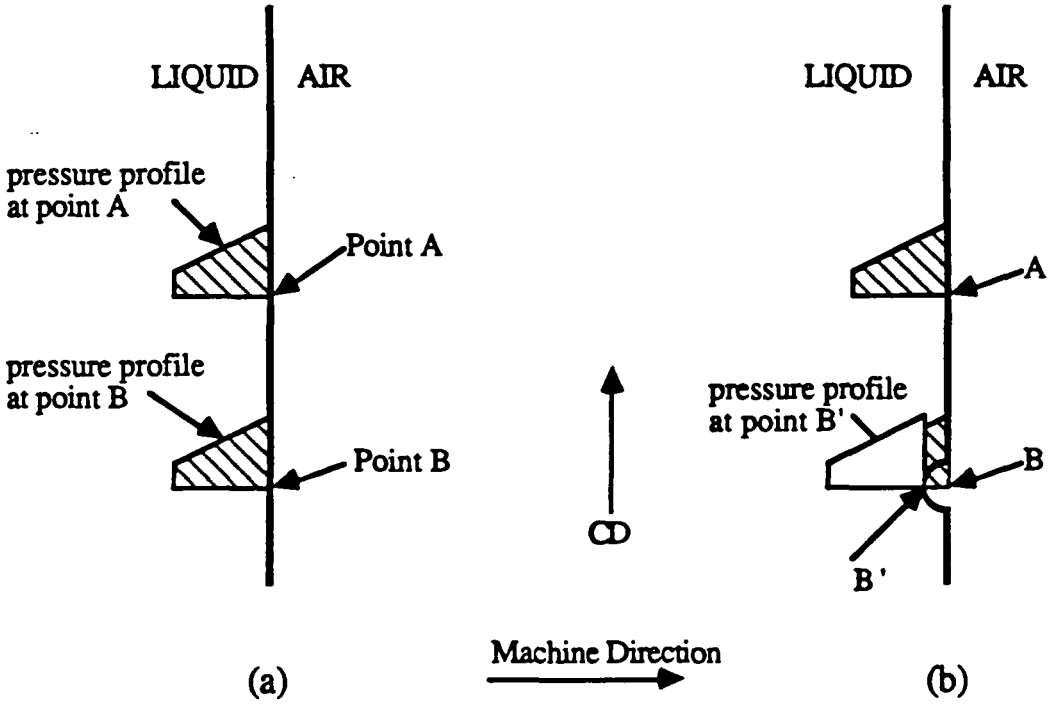

Figure II.10 Schematic of pressure profiles at an (a) undisturbed; and (b) disturbed meniscus between two parallel moving solid surfaces.

The fact that the meniscus in a forward roll coating is not always unstable (in contrast to Saffman and Taylor's model) indicates that the diverging surfaces of the rolls stabilize the flow at lower capillary numbers. The stabilizing mechanism is attributed to the change in the radius of curvature of the disturbed section of the meniscus. Since for diverging surfaces the free-surface at point B' in Fig. II.11 will have a smaller radius of curvatures than point A, this decrease in radius of curvature will reduce the pressure by an amount proportional to the surface tension. If the surface tension is large (small capillary number), then the decrease in pressure at the disturbed location due to reduction in radius of curvature will be greater than the increase due to the shift in pressure profile, and therefore, flow will be stable (Fig. II.11a). For large capillary numbers the influence of the surface curvature on the pressure will be small and the flow will become unstable (Fig. II.11b).

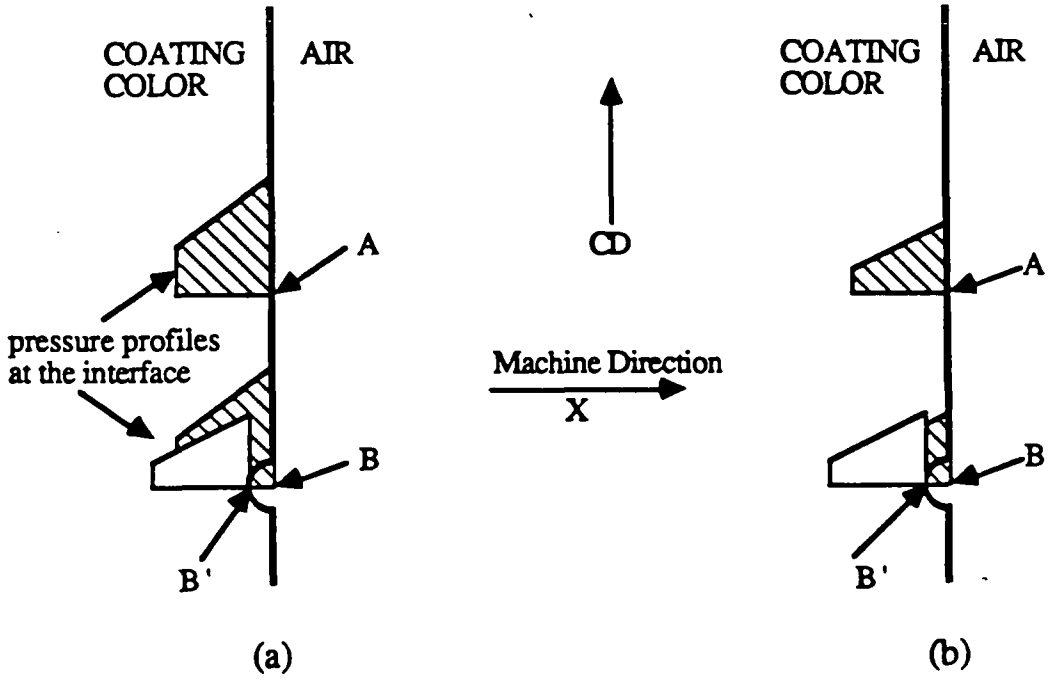

Figure II.11 Schematic of the pressure profile at the meniscus in forward roll coating (a) small capillary number; stable interface; and (b) large capillary number, unstable interface.

II.4 WETTING LINE INSTABILITY AND AIR ENTRAINMENT

In addition to flow instability and nonuniformities in coat weight distribution, most high-speed coating systems suffer from an additional constraint -- air entrainment at the contact line between liquid and the substrate. Air entrainment results in severe limitations on flexibility and speed of coating, and may form a bottleneck for the on-machine coaters.

The physics of dynamic wetting is not completely understood. In general, the contact line is a straight line where air, liquid, and solid meet. As the speed of the substrate increases, the contact angle approaches 180 degrees, at which point the contact line destabilizes and breaks into V-shaped (sawtooth) structures. The Vs grow in size with further increase in speed and finally air bubbles penetrate the liquid from the downstream tip of these structures. Flow visualizations of this process [34] show that two or more of these V structures coalesce, form and release a large bubble, and then resume their original shape in a time-periodic manner.

Currently, there is no theory which can fully explain the physics of wetting. The no-slip assumption at a solid wall results in a dynamic incompatibility in the system; the equations become singular at the wetting line. Various models (e.g., Navier slip condition) can be used in numerical simulations to treat the dynamic contact line in an approximate but consistent manner. A general background on contact angles and wetting is given in the review article by Dussan V. (1979). Recent progress in the understanding of dynamic wetting and air entrainment in thin film coating is given by Scriven (1990).

III. A GENERALIZED VIEW OF INSTABILITY AND BIFURCATION

Science is nothing without generalizations. Detached and ill-assorted facts are only raw material, and in the absence of a theoretical solvent, have but little nutritive value.

- Lord Rayleigh (1884)

Coating flows have complex (nonlinear) mechanical and dynamical characteristics. Application of coating on paper, by nature, demands flow through complicated coating devices from relatively low to very high shear regions. At the same time, a stable steady two-dimensional stream is often required at high speeds and *deviations* from this ideal situation may not be tolerated. It is these severe restrictions that demand better understanding of the dynamics and stability of the flow in coating devices. Under identical operating conditions, the flow in a short-dwell coater may be steady and nearly two-dimensional, steady three-dimensional, or unsteady three-dimensional. The conventional modeling methods and the classical approaches cannot fully explain and predict the physics of these problems. An explanation and generalization of the possible behaviors of the coating flows as dynamical systems is possible through simple nonlinear models and logical reasoning. This will provide the fluid mechanician and the engineer with a frame of reference and a guideline for cost-effective problem solving and improved systems designing. Bifurcation theory provides some of the tools that are required for this task. Results from simple experiments, such as flow visualization, can be used in conjunction with some fundamental principles of bifurcation to outline and predict very useful features of the system under study without actually performing extensive and costly experiments. A vivid example of this approach is Benjamin's (1978) analysis of bifurcation in steady flow of a viscous fluid flow in a circular Couette system.

In the following sections, we review some relevant and basic principles in bifurcation (one parameter) of equilibrium and periodic states of dynamical systems. The concepts are illustrated with simple mathematical models for clarification purposes. The subject matter is simple, yet it can be of enormous use when dealing with complex dynamical systems such as coating devices.

III.1 EQUILIBRIUM STATES

When two equilibrium solutions of a system of equations with distinct tangents intersect one another, the point of intersection is a singular point of bifurcation. In mathematical terms, let the system of nonlinear evolution equations be represented as

$$\dot{\underline{x}} = \underline{F}(\underline{x}, \lambda). \qquad \text{(III.1)}$$

where a dot over the dependent variables, $\underline{x}$, represents differentiation with respect to time and an underbar represents an n dimensional vector. Here λ is a parameter in the system and the analysis in this section is limited to a system of equations with only one parameter.

The equilibrium solutions of Eq. III.1 can be obtained from the system of equations given by

$$\underline{F}(\underline{x}(\lambda), \lambda) = \underline{0}. \qquad \text{(III.2)}$$

The dependent variables, $\underline{x}$, are functions of the parameter, λ. A regular point $(\underline{x}_r, \lambda_r)$ is a point where the Jacobian, $\underline{F}_{\underline{x}}(\underline{x}_r, \lambda_r)$, and $\underline{F}_{\lambda}(\underline{x}_r, \lambda_r)$ are not zero. The implicit function theorem [13] guarantees that a unique solution curve passes through a regular point.

Bifurcation theory deals basically with the study of the behavior of equilibrium solutions when the implicit function theorem breaks down. At the singular point $(\underline{x}_s, \lambda_r)$ where the determinant of $\underline{F}_{\underline{x}}(\underline{x}_s, \lambda_s)$ vanishes and $\underline{F}_{\lambda}(\underline{x}_s, \lambda_s) = 0$, the implicit function theorem is no longer valid.

A bifurcation point is a singular point at which two solutions of
Eq. III.2 intersect with a distinct tangent (double point). A simple example is the point U = 0, R = 5 in Fig. A.1 of the Appendix where two solutions, U = 0 and U = R - 5, intersect. As a second example, consider the evolution equation

$$\dot{U} = + U(\lambda - U^2). \qquad \text{(III.3)}$$

The two equilibrium solutions, U = 0, and $U = \pm\sqrt{\lambda}$ intersect at the origin. At the bifurcation point, the null solution, U = 0, loses stability and gives rise to a different stable solution. In other words, an exchange of stability takes place at the origin. The bifurcation

diagram is shown in Fig. III.1. When the bifurcating solution lies on the unstable/stable side of the trivial solution then it is termed *supercritical/subcritical.*

An example of a subcritical bifurcation is given by

$$\dot{U} = U\,(\lambda + U^2)$$

as shown in Fig. III.2. In contrast to the previous example, Eq. (III.3), here there is no exchange of stability at the origin, only a local loss of stability of the trivial solution.

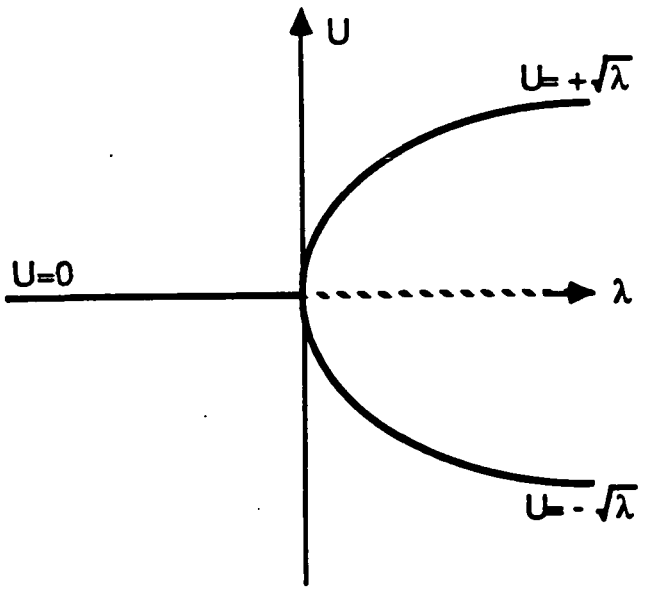

Figure III.1 A supercritical (pitchfork) bifurcation (one-sided).

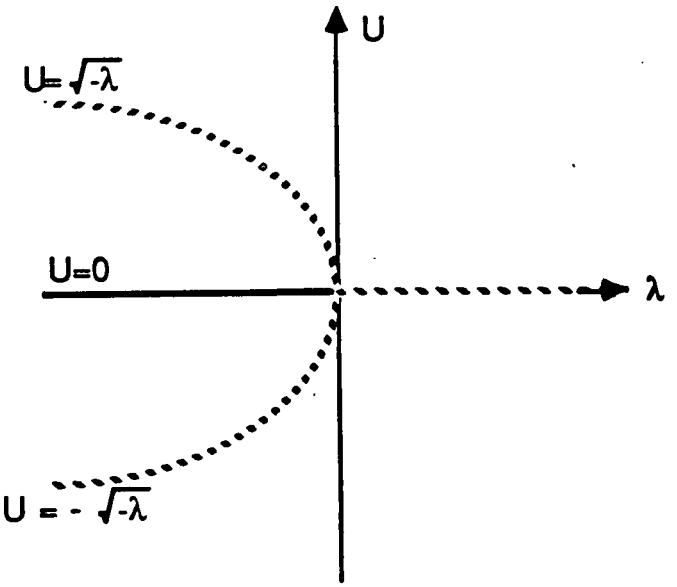

Figure III.2 A subcritical (pitchfork) bifurcation (one-sided).

A *transcritical* bifurcation occurs when the stable/unstable section of the bifurcating nontrivial solution is on the unstable/stable side of the bifurcation point of the trivial solution. Fig. A.1 in the Appendix is an example of a transcritical bifurcation. The following theorem summarizes the main results of a simple bifurcation point.

Theorem: Let i) $\underline{x} = \underline{0}$ be the trivial solution of $\underline{F}(\underline{x}, \lambda) = \underline{0}$ for all λ;

ii) $\sigma(\lambda)$ be a simple eigenvalue of $\underline{F}_{\underline{x}}(\underline{0}, \lambda)$;

iii) at the critical parameter, λ_c, eigenvalue,

$$\sigma(\lambda_c) = 0; \text{ and } \frac{d\sigma}{d\lambda}\Big|_{\lambda=\lambda_c} \neq 0,$$

then, 1) there is one and only one solution branch which intersects the trivial solution at λ_c;

2) the critical mode of a supercritical bifurcating solution is stable; and

3) the critical mode of a subcritical bifurcating solution is unstable.

III.2 TRANSITION FROM STEADY TO TIME-PERIODIC STATES

So far we have treated transitions between steady state solutions. Transition from steady to unsteady states will be treated in this section.

A transition to a time-periodic state can occur by at least two distinct mechanisms. In some dynamic systems, the steady state solution ceases to exist beyond the onset of time-periodicity where only an oscillatory solution can exist. In this case the transition occurs through a *turning point* in the steady state solution branch. An example of this transition is given by the simple model

$$\dot{U} = \sin U - \lambda \qquad \text{(III.4)}$$

where $0 \leq U \leq 2\pi$.

Two steady state solutions exist for $0 \leq \lambda \leq 1$. As shown in Fig. III.3, the stable and unstable equilibrium solutions meet at a turning point at $\lambda = 1$. Beyond this point for $\lambda > 1$, there are no steady solutions, only a time-periodic state for which frequency increases from zero at the transition point.

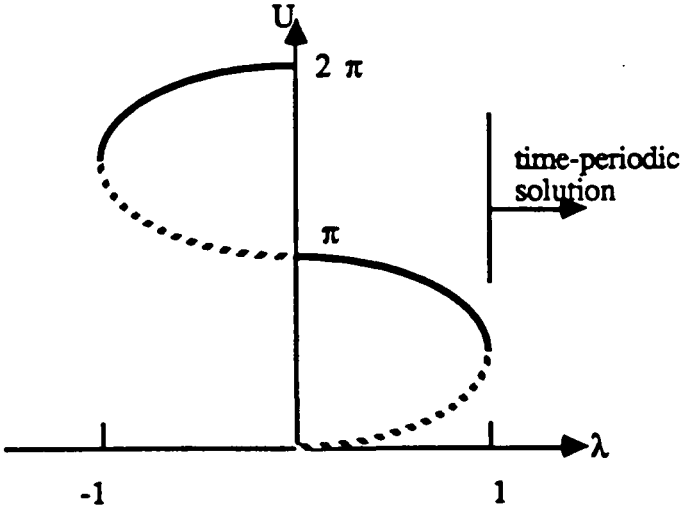

Figure III.3 Transition from steady to time-periodic state through a turning point.

The second mechanism for transition from steady to time-periodic state involves a loss of local stability of the steady state solution and exchange of stability to a time-periodic branch. The point where an equilibrium branch destabilizes and gives rise to a time-periodic branch is a *Hopf* bifurcation point. Let us consider a simple example of a Hopf bifurcation. Consider the system of evolution equations

$$\dot{U}_1 = -U_2 + U_1(\lambda - U_1^2 - U_2^2) \qquad \text{(III.5a)}$$

$$\dot{U}_1 = U_2 + U_1(\lambda - U_1^2 - U_2^2). \qquad \text{(III.5b)}$$

From the form of the equations, it is obvious that the trivial solution, $U_1 = U_2 = 0$, is the only equilibrium solution for all λ. Writing Eq. III.5 in local form, we can easily show that this solution destabilizes at $\lambda = 0$ and remains unstable for $\lambda > 0$. Although there is a

loss of stability at $\lambda = 0$, there is no turning point and no exchange of stability within the space of equilibria (no stationary bifurcation). The Jacobian has a pair of complex conjugate eigenvalues which cross the imaginary axis (with a nonzero speed) when $\lambda = 0$. To investigate this transition, let us reformulate system III.5 in polar coordinates R, θ defined as $R\cos\theta = U_1$ and $R\sin\theta = U_2$. After some manipulations, (III.5) reduces to

$$\dot{R} = R(\lambda - R^2) \qquad \text{(III.6a)}$$

$$\dot{\theta} = 1 \qquad \text{(III.6b)}$$

For $\lambda \geq 0$, the solution $R = \sqrt{\lambda}$ results in a time-periodic orbit, a *limit cycle*, given by $\theta = t$ and $R = \sqrt{\lambda}$. Therefore, the orbit has a period 2π and its amplitude (radius), as shown in Fig. III.4, grows with $\sqrt{\lambda}$. Since

$$\dot{R} < 0 \text{ for } R > \lambda$$

and

$$\dot{R} > 0 \text{ for } R < \lambda$$

the time-periodic state is stable, that is, all trajectories in the phase plane approach the limit cycle. The two branches of the equilibrium solution represent stable focus ($\lambda < 0$) and unstable focus ($\lambda > 0$) points. At $\lambda = 0$, a periodic solution bifurcates from the equilibrium branch and an exchange of stability from steady to time-periodic state takes place. In general, a Hopf bifurcation involves the crossing of the imaginary axis on the complex plane by a pair of complex conjugate eigenvalues of the Jacobian. The following theorem generalizing this transition was proved by E. Hopf (1942).

Theorem: Let i) x_0 be an equilibrium solution of the nonlinear system of equations $F(x, \lambda) = 0$ which destabilizes at $\lambda = \lambda_c$;

ii) The Jacobian $F_x(x_0, \lambda_0)$ has a simple pair of purely imaginary eigenvalues, $\mu(\lambda_0) = \pm i\beta$ and no other eigenvalues with zero real parts; and

iii) $\left.\frac{d\mu(\lambda)}{d\lambda}\right|_{\lambda=\lambda_0} \neq 0$, that is the crossing has nonzero speed;

then, 1) there is a bifurcation at (x_0, λ_0) to a unique (after fixing the phase) time-periodic solution branch;

2) the period of the limit cycle approaches $2\pi/\beta$ as λ approaches λ_0;

3) the bifurcating periodic branch is one-sided (transcritical bifurcations to periodic solutions are not possible) and the critical mode of a supercritical (subcritical) bifurcating solution is stable (unstable);

and,

4) Hopf bifurcation is generic, that is, small perturbations of the system of equations will not change the result qualitatively.

The exceptional bifurcation where multiple eigenvalues cross the imaginary axis or where transversality does not hold are discussed by Iooss and Joseph (1980).

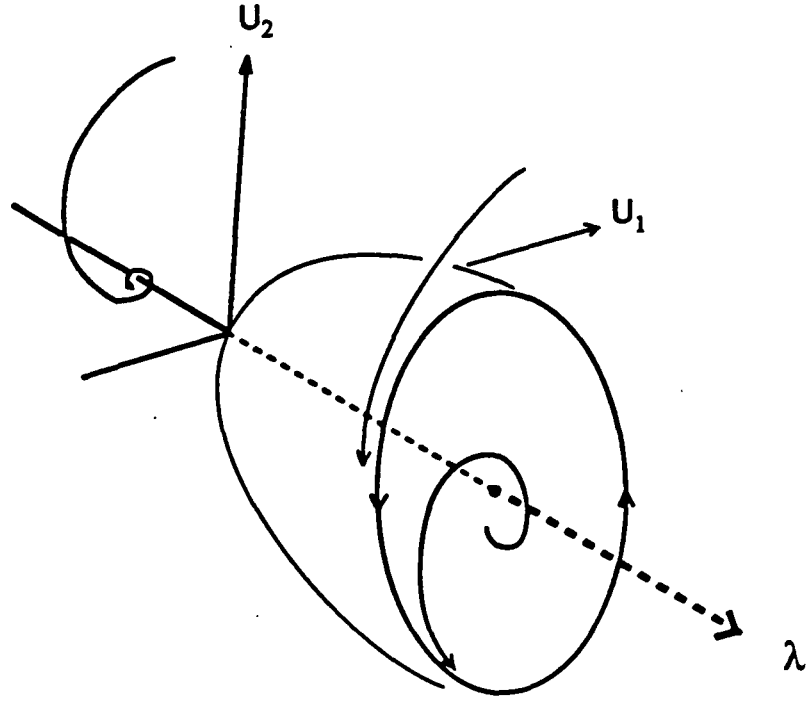

Figure III.4. Generation of stable limit cycles through a supercritical Hopf bifurcation.

The above example, Eq. III.5, illustrates a *supercritical* Hopf bifurcation where a *soft loss of stability* or *soft generation* of limit cycles occurs. In contrast, in the case of a subcritical

Hopf bifurcation, the periodic branch is initially unstable and turns back over the stable equilibrium branch (Fig. III.5). It then gains stability through a turning point at $\lambda = \lambda_1$. Between λ_1 and λ_0, there are three solutions: a stable equilibrium, a stable time-periodic, and an unstable time-periodic. As mentioned above, locally unstable states are not observable in real experiments and can be obtained only through computational analysis. A subcritical bifurcation with a subsequent turning point and transition to a stable state generates a bistable situation with *hysteresis* which is of considerable practical importance. Consider an experiment which is marching along the equilibrium branch of Fig. III.5 with gradually increasing control parameter, λ (the control parameter could be the machine speed, the Reynolds number, or any other parameter in the experiment which has primary influence on the dynamics). As λ approaches λ_0 there will be a sudden transition from steady state to a time-periodic state. In other words, at $\lambda = \lambda_0$ a *hard loss of stability* to a finite-amplitude time-periodic motion takes place. Now if the experiment marches backward on the periodic branch from $\lambda = \lambda_2$, it passes λ_0 without transitions until it reaches $\lambda = \lambda_1$. At this point the system jumps from the time-periodic state to a steady state and continues on the equilibrium branch as λ decreases.

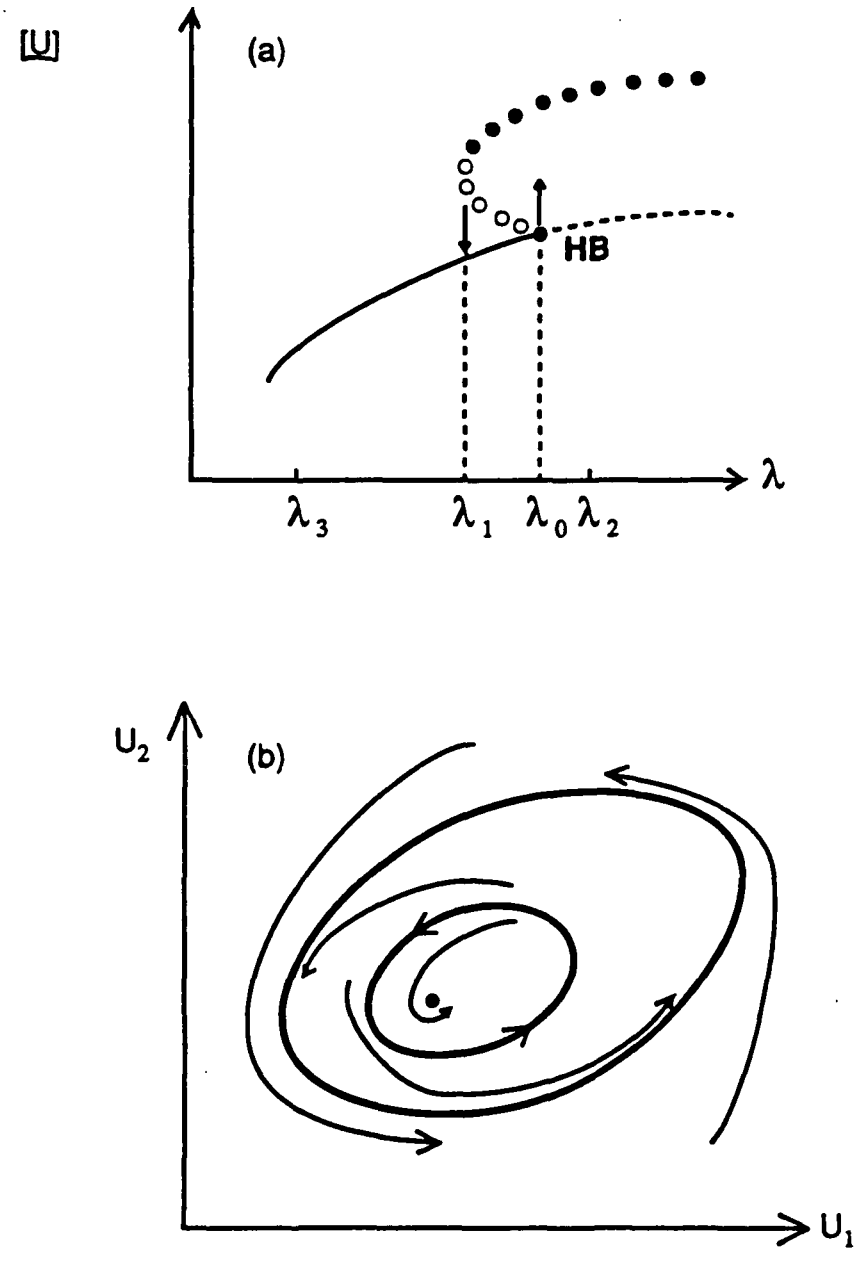

Figure III.5 Generation of stable and unstable limit cycles through a subcritical Hopf bifurcation; (a) bifurcation diagram where [U] is some scalar measure of the solution and open (closed) circles represent unstable (stable) time-periodic state; (b) stable and unstable limit cycles and the locally stable equilibrium point on the phase plane for $\lambda_1 > \lambda > \lambda_0$.

A Possible Explanation for the Dynamical Behavior of Short-Dwell Coaters at the Onset of Macroscopic Coat-Weight Nonuniformities (Streaks)

To demonstrate how the above information can be used to understand and explain the dynamics of coating systems, let us consider the problem of nonuniform coat weight distribution with short dwell coaters. Pilot trials show that within a specific range of machine speed and solids concentration the onset of streaks involves an intermittent behavior (not to be confused with the intermittency route to unsteady nonperiodic states). The coated surface shows patches of streaks followed by a relatively uniform coated region. What is causing this behavior? One possible mechanism is proposed below.

Consider a fluid flow experiment which exhibits the same dynamics as Fig. III.5, and which, due to some external effects (not necessarily flow dependent), is forced to oscillate between λ_3 and λ_2. Since a bistable situation exists in the subinterval λ_0 to λ_1 in combination with the hysteresis effect generated by the subcritical Hopf bifurcation, a *bursting* phenomenon will be observed in the experiment. During the pass from left to right along the equilibrium branch as λ increases from λ_3 to λ_0, the flow is stationary (steady) and uniform. As the control parameter passes λ_0, the system jumps to the periodic branch. This generates initial transients which could involve several large amplitude oscillations which could persist until λ approaches λ_3. The alternatively active and stationary modes of the flow result in periodic bursts. This dynamical behavior has also been observed in other experimental and industrial applications (for an example see Rinzel and Troy, 1982).

Transition from the primary steady-state to a time-periodic state with small oscillation amplitude has been observed in the flow of Newtonian fluids in a lid-driven cavity simulating the pond of a short-dwell coater. Although not rigorously proved yet, this transition is most likely to be through a Hopf bifurcation (section III.2). Considering the fact that the additional force introduced by the elasticity of the fluid makes a subcritical Hopf bifurcation possible, the mechanism proposed above becomes viable.

Here, the whole coating system is considered a dynamical unit with multiple parameters. The parameter which may drive this unit to oscillate through the critical region, λ_3 to λ_2, could be, for example, the periodic shear-induced pigment structures (bridges) that may

form under the blade, the hydrodynamic effects upstream of the blade, or even some mechanical property of the system.

By pinpointing the mechanism and the parameters which destabilize and control the coating system, we can design a more stable, reliable, and cost-effective device.

ACKNOWLEDGEMENT

This work was supported by the member companies of The Institute of Paper Science and Technology through Project 3674 - Fundamentals of Coating Systems. Constructive comments and useful suggestions by Professor L.E. Scriven on an earlier version of this paper are gratefully acknowledged.

LITERATURE CITED

1. Aidun, C.K., and Triantafillopoulos, N.G., "Global stability properties of flow structures in the pond of a short-dwell blade coater," Int'l Symp. Mech. of Thin-Film Coating, AIChE Meeting, March 18-22, 1990.

2. Benjamin, T.B., "Bifurcation Phenomena in Steady Flows of a Viscous Fluid," *Proc. Roy. Soc.* **A 359**, 1, 1978.

3. Brewster, D.B., and Nissan, A.H., "Hydrodynamics of Flow Between Horizontal Concentric Cylinders. I. Flow Due to Rotation of Cylinder," *Chem. Eng. Sci.*, **7**, 215, 1958.

4. Brewster, D.B., Grosberg, P., and Nissan, A.H., "The Stability of Viscous Flow Between Horizontal Concentric Cylinder," *Proc. Roy. Soc.* **A251**, 76, 1959.

5. Burkhalter, J.E., and Koschmieder, E.L., "Steady Supercritical Taylor Vortex Flow," *J. Fluid Mech.*, **58**, 547, 1973.

6. Christodoulou, K.N., "Computational Physics of Slide Coating Flow," Ph.D. Thesis, University of Minnesota, 1990.

7. Dean, W.R., "Fluid Motion in a curved channel," *Proc. Roy. Soc.*, **A 121**, 402, 1928.

8. Dussan V., E.B., "On the Spreading of Liquid on Solid Surfaces: Static and Dynamic Contact Lines," *Ann. Rev. Fluid Mech.*, **11**, 371, 1979.

9. Eklund, D.E., "Review of Surface Application," Trans. of the Ninth Fund. Research Symp., ed. Baker and Punton, Mech. Eng. Pub., 1989.

10. Fjortoft, R., "Application of Integral Theorems in Deriving Criteria of Stability for Laminar Flows and for the Baroclinic Circular Vortex," *Geofys. Publ., Oslo* **17**, No. 6, 1, 1950.

11. Görtler, H., "On the Three Dimensional Instability of Laminar Boundary Layers on Concave Walls," *Nachr. Ges. Wiss. Gottingen*, N.F. 2, No. 1, 1940.

12. Higgins, B.G., "Dynamics of Coating, Adhesion and Wetting," Status Report 3328, Institute of Paper Science and Technology (former Institute of Paper Chemistry), October 20, 1981.

13. Iooss, G., Joseph, D.D., Elementary Stability and Bifurcation Theory, Springer-Verlag, New York, 1980.

14. Kistler, S.F. and Scriven, L.E. "Coating Flows," In Computational Analysis of Polymers, ed. J. Pearson, S. Richards, Chap. 8, Barking, Essen. Engl.: Appl. Sci. 343, 1983.

15. Landau, L.D.; and Lifshitz, E.M., Fluid Mechanics, vol. 6 of course on theoretical physics (Translated from Russian by J.B. Sykes and W.B. Reid) London: Pergamon Press, 1959.

16. Lin, C.C., The Theory of Hydrodynamic Stability, Cambridge University Press, 1955.

17. Orr, W. M.F., "The Stability or Instability of the Steady Motions of a Perfect Liquid and of a Viscous Liquid," *Proc. Roy. Soc. Irish Acad.* **A 27**, 9, 1907.

18. Pitts, E., and Greiller, J., "The Flow of Thin Liquid Films Between Rollers," *J. Fluid Mech.*, **11**, 33, 1961.

19. Pranckh, F.R., and Scriven, L.E., "The Physics of Blade Coating of Deformable Substrate," 1988 Coating Conference Proc., TAPPI Press, Atlanta, GA, 1988.

20. Raney, D.C., and Chang, T.S., "Oscillatory Modes of Instability Between Rotating Cylinders With a Transverse Pressure Gradient, *Z. Agnew Math. Phys.* **22**, 680, 1971.

21. Rayleigh, Lord, "On the Instability of Jets," *Proc. London Math. Soc.* **10**, 4, 1879.

22. Rayleigh, Lord, "On the Stability, or Instability, of Certain Fluid Motions," *Proc. London Math. Soc.* **11**, 57, 1880.

23. Reynolds, O., "An Experimental Investigation of the Circumstances Which Determine Whether the Motion of Water Shall be Direct or Sinuous, and of the Law of Resistance in Parallel Channels," *Phil. Trans. Roy. Soc.* **174**, 935, 1883.

24. Ruschak, K.J. , "Coating Flows," *Ann. Rev. Fluid Mech.*, 17, 65, 1985.

25. Ruschak, K.J., "Boundary Conditions at a Liquid/Air Interface in Lubrication Flows," *J. Fluid Mech.*, **199**, 107, 1982.

26. Saffman, P.G., and Taylor, G.I., "The Penetration of a Fluid into a Porous Medium or Hele-Shaw Cell Containing a More Viscous Liquid," *Proc. Roy. Soc. London*, Ser A, **245**, 312, 1958.

27. Schweizer, P.M., and Scriven, L.E., "Evidence of Görtler-Type Vortices in Curved Film Flows," *Phys. Fluid*, **26**, 619, 1983.

28. Scriven, L.E., "On the Physics of Dynamic Wetting and Air Entrainment," Int'l Symp. Mech. of Thin-Film Coating, AIChE Meeting, March 18-22, 1990.

29. Sommerfeld, A., "Ein Beitrag zur Hydrodynamischen Erklaerung der Turbulenten Fluessigkeitsbewegungen," *Proc. 4th International Cong. Mathematicians*, **III**, 116, 1908.

30. Squire, L.C., "On the Stability of Three-Dimensional Disturbances of Viscous flow between Parallel Walls," *Proc. Roy. Soc.* **A 142**, 621, 1933.

31. Steen, P.H., and Aidun, C.K., "Time-Periodic Convection in Porous Media: Transition Mechanism," *J. Fluid Mech.*, **196**, 263, 1988.

32. Synge, J.L., "Hydrodynamical Stability," Semi-centenn. Publ. Amer. Math. Soc., **2**, 227, 1938.

33. Taylor, G.I., "Stability of a Viscous Liquid Contained Between Two Rotating Cylinders," *Phil. Trans. Roy. Soc.*, **A223**, 289, 1923.

34. Veverka, P., "Dynamic Contact Line Instability and Air Entrainment," Masters Thesis (in progress), Institute of Paper Science and Technology, Atlanta, GA, 1990.

APPENDIX I

The conservation principles in fluid mechanics can be written in the form of a system of differential equations which govern the basic motion of the fluid. These equations, as they stand, cannot predict the stability properties of the base flow. To examine stability, a disturbance can be imposed on the base flow and the resulting equations will show if the disturbance grows (unstable) or decays (stable). For illustration purposes, assume that the equation

$$\frac{dU}{dt} = - U (U - R + 5) \qquad (A.1)$$

governs a system with dependent variable U. R is a real number which serves as the parameter (such as Reynolds number) in the problem. The steady state solutions to this equation can be found by setting $\frac{dU}{dt} = 0$ and solving the algebraic equation

$$U (U - R + 5) = 0 \qquad (A.2)$$

Therefore, U=0 and U = R-5 are each an equilibrium solution of the evolution Eq. A.1. But which solution is stable and can physically exist ? To answer this question, we examine the stability of each solution by analyzing the behavior of that solution with respect to an infinitesimal disturbance. More specifically, we study the behavior of $U+ \varepsilon u(t)$, where $\varepsilon u(t)$ is an infinitesimal disturbance. Substituting the disturbed solution into Eq. A.1, it is easy to show that the disturbance, u(t), imposed on the base solution, U, behaves as

$$u(t) = \exp (st),$$

where the growth parameter, s, is given by

$$s = -[2U - (R - 5)].$$

Depending on the magnitude of R, the parameter s could be positive or negative and result in unstable or stable solutions, respectively.

For the base solution, U = R - 5, the disturbance u(t) grows when R<5 and decays when R>5. This solution is therefore unstable when R<5 and it stabilizes at the critical value, R_c=5.

The null solution, U=0, is stable when R<5, destabilizes at R=5, and remains unstable for R>5.

These results are summarized in Fig. A.1 where stable and unstable solution branches are shown with solid and broken lines, respectively. This analysis shows that for R<5, the only physically possible state is U=0, and for R>5, U=R-5 is the only stable state.

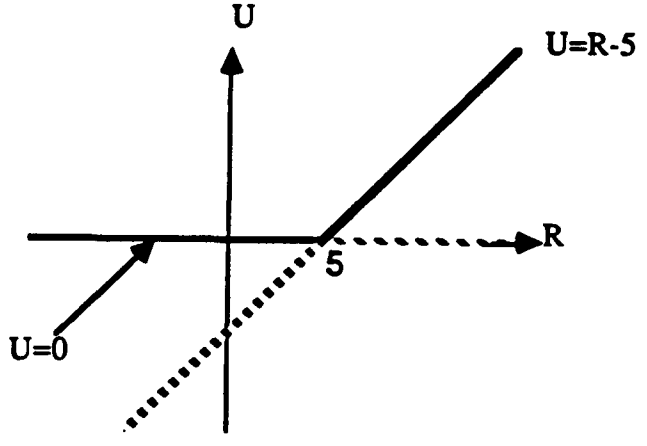

Figure A.1 Stability characteristics of the solutions U=) and U=R-5.